Regular Article

Marcin Graba* and Andrzej Grycz

Application of finite element method in industrial design, example of an electric motorcycle design project

https://doi.org/10.1515/eng-2022-0569 received August 23, 2023; accepted November 27, 2023

Abstract: This study presents the use of finite element method (FEM) in solving the real engineering problems, e.g., an electric motorcycle design project. A simplified scheme of industrial design is presented, followed by an indication of how to use the capabilities of the selected CAD/CAM/ CAE software in the industrial design of industrial form. Using concurrent design based on the CAD system with the simultaneous use of CAE modules, the interdisciplinary of industrial design engineering was shown, which cannot exist without access to numerical methods. In the electric motorcycle project discussed in this article, the close relation between CAD and CAE modules was used, looking for the best solution in the construction of the motorcycle frame. By conducting a series of numerical simulations based on the FEM and topological optimization, the final shape of the frame and the rear control arm mounting was presented. The designed structure was optimized in terms of mass and effective stress distributions determined from the Huber-Mises-Hencky hypothesis. The resulting model of the frame was adapted to the design project, briefly discussed in the summary of the article. This study indicates the need to use the FEM and CAD/CAM/CAE applications at almost every stage of engineering design.

Andrzej Grycz: Department of Metrology and Non-conventional Manufacturing Methods, Faculty of Mechatronics and Mechanical Engineering, Kielce University of Technology, Aleja Tysiąclecia Państwa Polskiego 7, 25-314 Kielce, Poland, e-mail: andrzewszymongrycz@gmail.com

Keywords: design, 3D modeling, industrial design, FEM, topological optimization, stress distributions, strain distributions, CAD/CAM/CAE systems

1 Introduction

The current century, twenty-first century, so far, is a period of significant cultural, technological, and ideological changes. The ease of obtaining and transmitting information contributes to progress in many areas of life, including the development of methods of movement. This is manifested by the popularization of electric vehicles and the development of motorized personal transport vehicles.

Electric motorcycle designs have been around since the nineteenth century, but they were mostly vehicles designed for racing or breaking speed records. The first electric motor-powered two-wheeled vehicle available to consumers did not appear until 2006, in the form of the Vectrix VX-1 scooter. The successors of the VX-1 model were the VX-2 scooters and the VX-3 tricycle. The company ceased its operations in 2014 [1].

The first commercially available electric motorcycle was the Zero S by Zero Motorcycles, introduced in 2009. It had a top speed of 158 km/h and a range of 143 km. Zero S, after the changes carried out in 2014 and 2020, is still in production [2,3].

Until 2018–2020, the electric motorcycle market developed slowly. As a result of the popularization of other types of electric vehicles, as well as social movements aimed at eliminating internal combustion engines, the automotive industry has developed very rapidly over the last 2 years, resulting in a gradual saturation of the market and the appearance of numerous models with different specifications and types of frame construction. This prompted the authors of this study to present their own concept of a new vehicle powered by electricity [4].

The idea of the project [4], implemented in 2020–2021 at the Faculty of Mechatronics and Mechanical Engineering of

^{*} Corresponding author: Marcin Graba, Department of Metrology and Non-conventional Manufacturing Methods, Faculty of Mechatronics and Mechanical Engineering, Kielce University of Technology, Aleja Tysiąclecia Państwa Polskiego 7, 25-314 Kielce, Poland, e-mail: mgraba@tu.kielce.pl

the Kielce University of Technology, was the graphic and construction development of an electric motorcycle, combining the advantages of communication methods attributed to electric vehicles, along with increasing the level of user safety in relation to many electric vehicles. In addition, it was assumed that the vehicle should be the most ergonomic product, exceeding the available commercial solutions in this parameter. The basis of the concept was to design a replacement vehicle for a car for the widest possible audience, mainly residents of cities and suburban areas, while maintaining a recognizable and socially acceptable motorcycle style. The possible introduction of the vehicle to the market is intended to reduce air pollution and noise, promote the appearance and performance of ecological solutions and reduce the area required for the use, and parking of the vehicle. In the spirit of "function follows form," the key assumption was to design a vehicle geometry that would allow its functional features to be fully exploited.

An outline of design, leading to the presentation of a new industrial form of an electric motorcycle, is presented in Section 2. The principles of designing industrial forms are briefly presented in Section 3, which have been largely supplemented with numerical calculations carried out using the finite element method (FEM), which allowed the optimization of selected components of the designed structure. This study is a proof of the interdisciplinarity of broadly understood industrial design and its close relationship with engineering design and the CAD/CAM/Computer Aided Engineering (CAE) systems used in it.

2 Brief reflections on the prepared preliminary design of the electric motorcycle

In order to simplify subsequent activities in the entire design process, a product synthesis scheme was used, describing the individual determinants of the project. This scheme was given by Eskild Tjalve in the textbook "A Short Course in Industrial Design" [5]. Figure 1 shows in a simplified way the steps taken during the design process, which change depending on the stage of the project.

Having strictly defined criteria and an analysis of the design problem, it is necessary to consider the basic structure, which describes the general principle of operation of the structure, and presents components and their functions. In practice, this refers to drawing a simplified diagram of the designed industrial form. In the undertaken

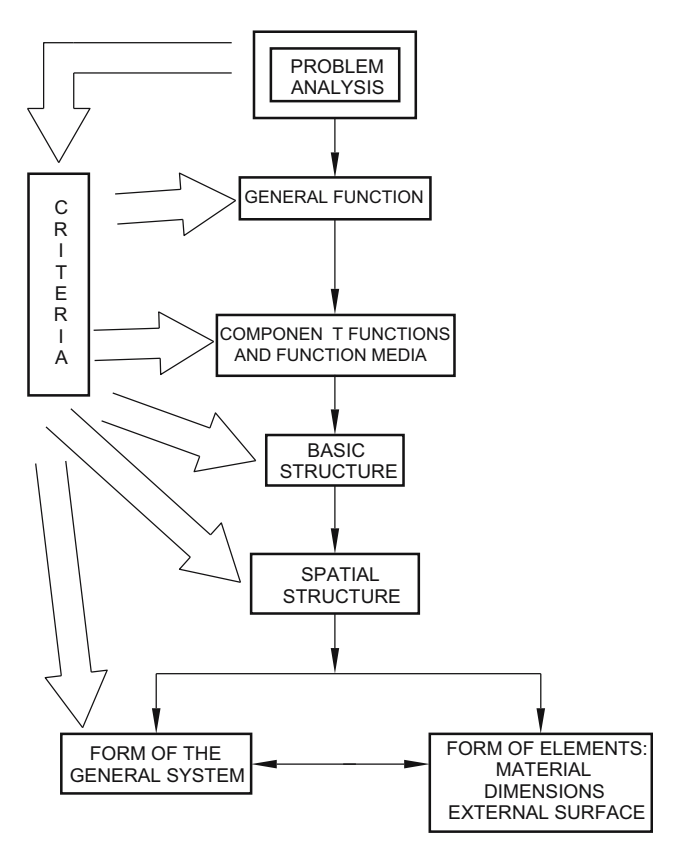


Figure 1: Scheme of product synthesis (own study based on [5]).

design problem, the design of an electric motorcycle, there are many subsystems of elements: the drive system, the braking system, the steering system, etc. Due to this, only the drive control system of the proposed electric motorcycle model will be presented, defining the general function (Figure 2).

As can be seen in Figure 2, the user, using the knob (1), sends information about the intention to set the vehicle in

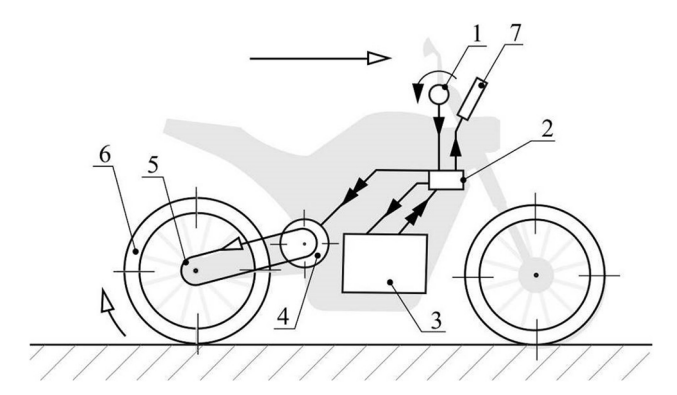


Figure 2: Simplified diagram of drive control: 1 – knob; 2 – control system; 3 – indicators; 4 – battery; 5 – drive unit; 6 – gear; and 7 – drive wheel (own study based on [4]).

motion to the control system (2), then the control system sends a request for the transport of electricity to the controller connected to the battery (3), which in the next step transmits electricity to the motor (4), which sets the gear (5) in motion. The transmission transmits the drive torque to the drive wheel (6), which, acting on the ground, sets the vehicle in motion. The control system sends information to the indicators (7), which inform the user about the speed of the vehicle, battery charge level, and other data. In Figure 2, the shaded arrows indicate the direction of information transfer, double arrows indicate the direction of electricity transmission, and empty arrows indicate the direction of movement.

Based on a series of different possible solutions, not quoted in this article, the arrangement of the most important elements of the motorcycle was proposed, as shown in Figure 3. The conventional variation of the motorcycle's

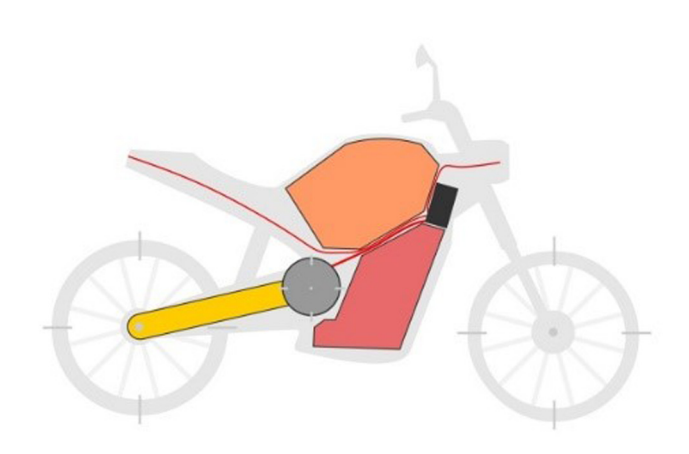


Figure 3: Conventional variation of the selected construction solution of the motorcycle with the designation of the main components using different colors (gray color – drive unit, black color – components controlling the vehicle, red color – battery, yellow color – chain transmission/drive shaft, orange color – clipboard, cable connections are marked with red lines.

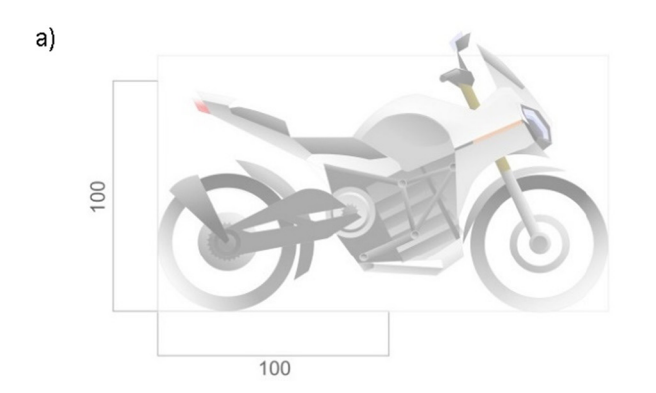
design solution shown below places the engine under the seat, changing the visual weight of the body. Finally, it was decided to combine the motor, battery, and drive unit into one subassembly, protected by a shell. The use of a drive chain slightly increases the weight and reduces the efficiency, but this is a decision related to fashion and visual issues. The structure of the shown variation, allows for the largest storage capacity, which translates into the possibility of storing a motorcycle helmet. This is a solution that significantly improves the ergonomics of the vehicle.

Having predetermined the basic structure, in the next step, the form of the general system was defined in the design project, which in short means the final form of the entire industrial form, i.e., its appearance, dimensions, and external surface of the pattern. In the discussed electric motorcycle project, the focus was on the following:

- appearance, characterized by a streamlined body, mixing soaring geometry with rounded shapes;
- different color variants, mixing 2–3 separate shades;
- · minimalist decals applied to the varnish.

The vehicle length was assumed to be approximately 2,000 mm, the tank height measured from the ground was not exceeding 1,000 mm, and the seat height measured from the ground was less than 800 mm. The outer surface is supposed to be smooth, covered with glossy or matte varnish (Figures 4–6).

Defining the form of the most important components of the motorcycle in the next step, it was decided that the wheels would be made of a light shoulder construction, with a diameter of 16 in, and the width of the wheels would be in the range of 80–110 mm. The whole will be complemented by dark colors, slightly shiny or matte surface. The rims will be made of aluminum alloy. The bodywork, which is the appearance of a motorcycle, will be based on the scheme of the vehicle's skull connected to the headlight. The bodywork forms an envelope around the steering



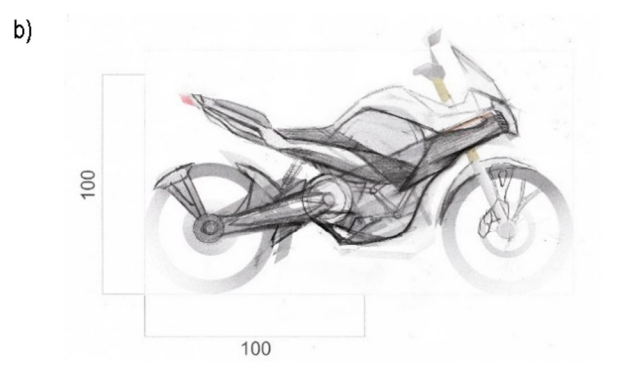


Figure 4: (a) Graphic design base and (b) electric motorcycle – freehand sketch of the motorcycle frame.

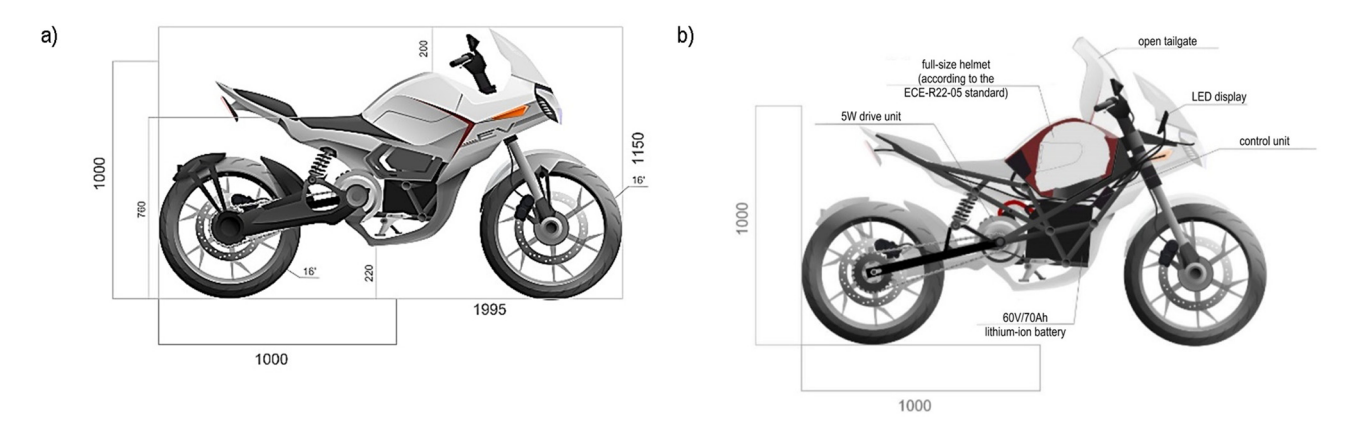


Figure 5: (a) Electric motorcycle – I variant sketch and (b) electric motorcycle – design sketch of variant I.

wheel. Sharp geometry on the body side line is used, as well as a uniform color across the entire surface and minor color accents. The surface of the car body will be smooth, matte, or glossy, covered with varnish. The construction material of the car body can be fiberglass or properly selected plastic. The load-bearing element of the vehicle, the frame, is to be made of steel or aluminum pipes, which will reduce the weight of the vehicle. Among other elements that determine the appearance of the designed industrial form, one cannot fail to mention the seat, which should be made of leather or synthetic fabric material in dark gray. Another element is LED lighting and a color LED display located in a plastic structure (Figures 4–6).

Designing in accordance with the principles of universal design, it was assumed that an important element in the project is the renewability and low cost of production of structural elements. Therefore, it was envisaged that aluminum and magnesium alloy AlMg3Mn - 5454-

H111, characterized by corrosion resistance and increased strength, would be used for the wheel rims of the designed motorcycle. The vehicle frame, which is the subject of further consideration, will be made of the AlZnMg - 7050-T7351 alloy, characterized by a high yield strength (435 MPa), in order to reduce the weight in relation to the initially planned steel pipes. The project will also use the S235JR structural steel alloy, which was selected as the material for the protective shell of the battery and as the material for the elements of the motorcycle suspension structure.

Based on the information provided above, a preliminary graphic design of the designed industrial form was developed (Figure 4a), which was verified in order to determine the shape of the frame (Figure 4b).

On the basis of the graphic design base and the designated lines in the freehand sketch, vector graphics were created showing the initial concept of the industrial design on a scale of 1:10 (Figure 5a). In the next step, an exemplary

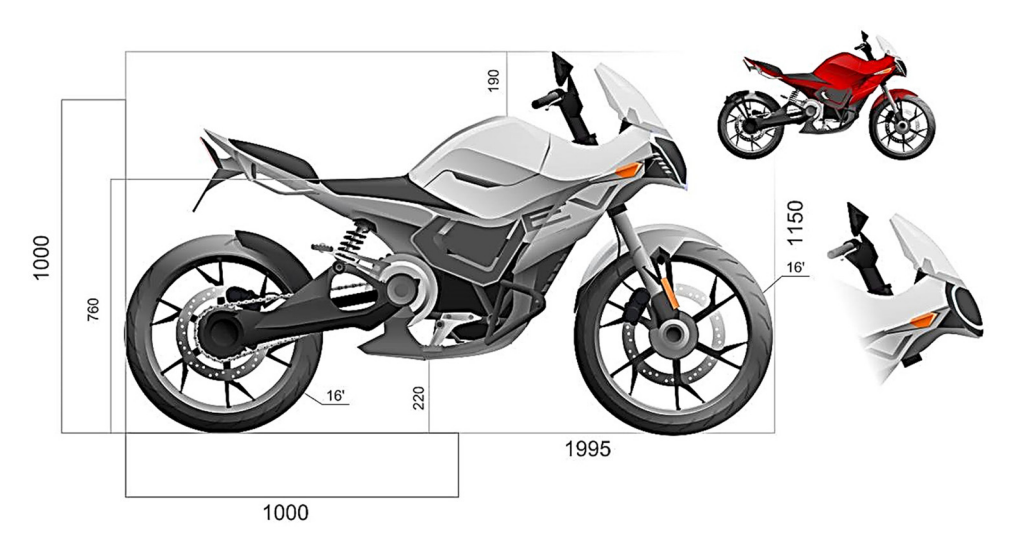


Figure 6: Electric motorcycle – sketch of variant II.

vehicle structure was drawn in order to better illustrate the arrangement of individual components (Figure 5b). Subsequently, changes were made to the design to achieve a smoother geometry, greater consistency of form, and an overall improvement in visual values (Figure 6).

The next stage of developing the industrial design was to create a virtual spatial model of the product. Making a spatial model is one of the most important elements of the design process, because it allows you to visualize the actual geometry of the pattern and analyze various parameters, such as dimensions, weight, area, strength, and others. The CAD software can be used for this purpose, or vector geometry programs can be used to obtain only geometry without the possibility of analysis. The following modeling process was based on the use of the SOLIDWORKS 2019 application [6], enabling a wide range of engineering activities - from graphic design to optimizing the structure using the FEM. In Section 3, the use of the FEM in industrial design will be discussed, e.g., in creating a spatial model of the vehicle frame structure, i.e., determining its geometry, checking technical parameters, and performing the FEM analysis [7], along with topographic optimization, in order to improve the strength of the support element that fastens the rear swingarm, while maintaining the relative weight of the element.

3 Designing and modeling the vehicle frame using FEM analysis

The chassis, i.e., in relation to two-wheeled vehicles more often used, the frame, is one of the most important structural elements of motorcycle construction. It is an element that connects all vehicle components, transfers the stresses resulting from the weight of the vehicle and users to the

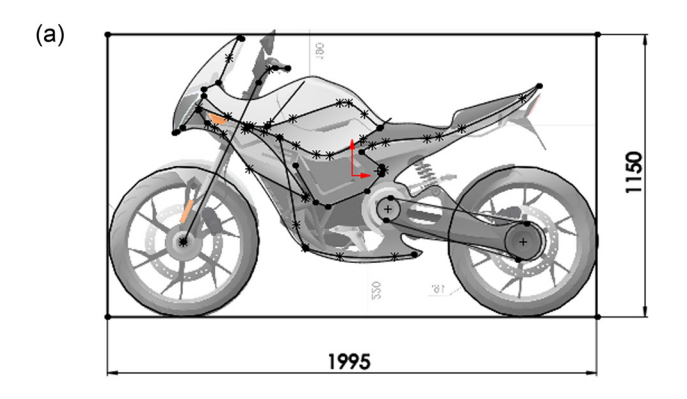
suspension elements. It is also responsible for the stiffness of the structure and its behavior under the influence of external forces. Frame parameters are often a determining factor in handling, driver and passenger positions, as well as the strength and overall behavior of a vehicle in the event of a collision.

It should be noted that in fact the process of constructing this element in each of the motorcycles takes months or even years, it also requires a specialized team of constructors, analyzing and testing the achieved results, and then changing the geometry, improving mechanical properties, and adjusting the cost and production method at the same time. It is also a process to be carried out simultaneously with the construction of other vehicle components, such as suspension, bodywork, etc. For the needs of the presented project, however, it is possible to outline the approximate shape of the structure and optimize the mass based on the assumptions made.

Some of the following assumptions were developed on the basis of the manual for the construction of motorcycle vehicles "Motorcycle Handling And Chassis Design" by Tony Foale, published in electronic form in 2002 [8].

3.1 CAD design of the frame and selected elements of the motorcycle structure

The first assumption is to match the frame structure to the shape and dimensions of the drive unit described above. Due to the nature of the work, the shape and overall dimensions of the subassembly, as well as its position in the mold, were assumed. For this purpose, in the SOLIDW-ORKS application [6], using the 3D Sketch tool, the general lines of the vehicle were drawn, which will serve as the basis for the construction (Figure 7).



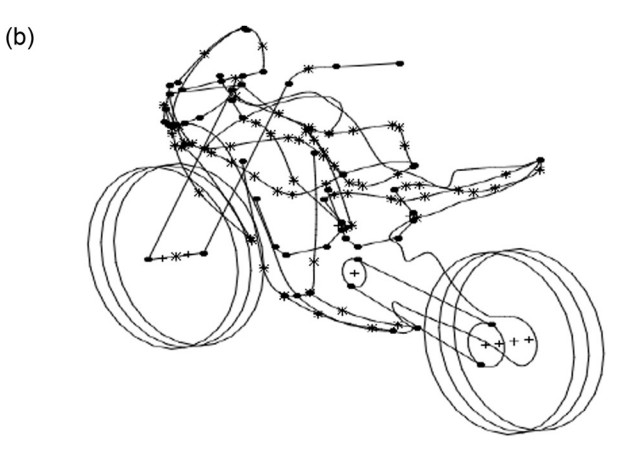


Figure 7: (a) Spatial diagram of the vehicle in a flat projection and (b) spatial diagram of the vehicle in an axometric projection.

Then, a model of the drive unit was created and placed inside the body of the vehicle, adjusting the positions of individual components in the shell (Figure 8).

In Figure 9, red areas mark the connection surfaces of the assembly with the vehicle frame. These are holes for M15 and M8 screw connections. Based on the shape of the frame, the position of the additional M15 connection is determined, connecting the side surface of the shell with the frame. The engine will be connected directly to the frame, using bolts, also connecting it to the shell (Figure 9).

The task of the frame is to hold the subassembly, which is also a structural part, transmitting stresses. The load should not generate stresses in the frame exceeding the value determined on the basis of the safety factor. The mass of the assembly was estimated by estimating the masses of individual elements.

In the case of batteries, the energy to weight ratio for lithium-ion batteries is approximately 100–250 Wh/kg [9]. For simplicity, the value is averaged to 175 Wh/kg. Assuming that the battery is to have a capacity of 4 kWh, we can use the following simple equation to determine the mass:

$$m_{\rm battery} = \frac{4,000 \text{Wh}}{175 \frac{\text{Wh}}{\text{kg}}} \approx 23 \text{ kg},$$
 (1)

where m_{battery} is the weight of the battery used in the motorcycle.

The resulting mass of 23 kg was raised to 25 kg, assuming cell connections, transformer, and other components. The density of lithium-ion batteries is approximately ~2,000 kg/m³ [10]. Using this fact, the volume of the battery solid was calculated, amounting to about 1.15×10^7 mm³, and a similar volume value was used in the construction of the battery model.

In the case of the engine, a mass of 12 kg was assumed after analyzing available commercial solutions. The same was done for the controller, assuming a mass of 2.5 kg,



Figure 9: Drive unit in axometric projection with connection surfaces for connecting to the vehicle frame (marked by red).

consisting of cables and other components. The mass of the cooler after the analysis of commercial solutions is 8 kg, which consists of the mass of pipes and coolant. For the shell, using S235JR material for the component, a weight of 4.92 kg was achieved. The final value was assumed as 5.5 kg, including fixings and other structural elements. This resulted from the shell design process and the estimation made in the SOLIDWORKS 2019 application [6]. The shell model is shown in Figure 10.

Summing up the abovementioned values, it can be written that the final mass of the component is:

$$m_{\text{component}} = 25 \text{ kg} + 12 \text{ kg} + 2.5 \text{ kg} + 8 \text{ kg} + 5.5 \text{ kg}$$

= 53 kg. (2)

Multiplied by the gravitational constant of approximately g = 9.81 N/kg, the weight of the component is

$$Q_{\text{component}} = 53 \text{ kg} \cdot 9.81 \frac{\text{N}}{\text{kg}} = 519.93 \text{N}.$$
 (3)

From the above calculations, it follows that the load Q = 520 N, with vectors attached to the surfaces of the connection between the frame and the battery, should

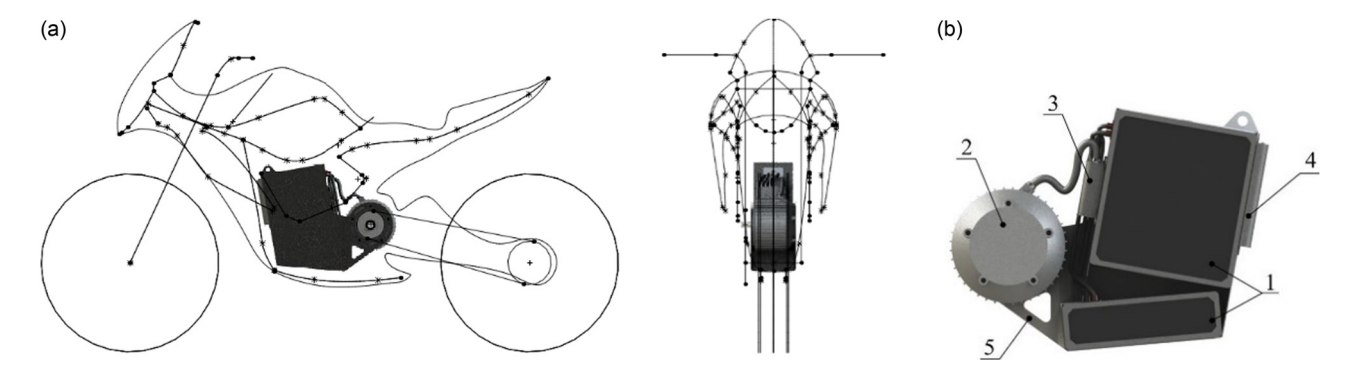


Figure 8: (a) Position of the drive unit inside the vehicle in plan views and (b) drive unit components: two batteries (1), motor (2), controller (3), radiator (4), and a shell covering the entire subassembly (5), made of 2 mm thick S235JR steel sheet.



Figure 10: Model of the shell next to the drive system of the designed motorcycle.

generate stresses lower than the yield strength of the material, divided by the adopted safety factor. It should also be noted that due to the above simplifications and assumptions, the actual force may slightly differ from the given value.

After determining the mass of the system, it is necessary to determine the weight of the users: the driver and the passenger. Assuming the total mass of passengers to be 200 kg, including additional loads such as clothes or hand luggage, the force directed along the vertical axis of the system is

$$Q_{\text{users}} = 200 \text{ kg} \cdot 9.81 \frac{\text{N}}{\text{kg}} = 1,962 \text{N}.$$
 (4)

In practice, this means that a static load of Q = 2,000 N fixed on the seat surface (Figure 11) should not generate stresses exceeding the permissible stresses.

In the next step, the angle of inclination of the front fork was determined. Determining the angle of inclination

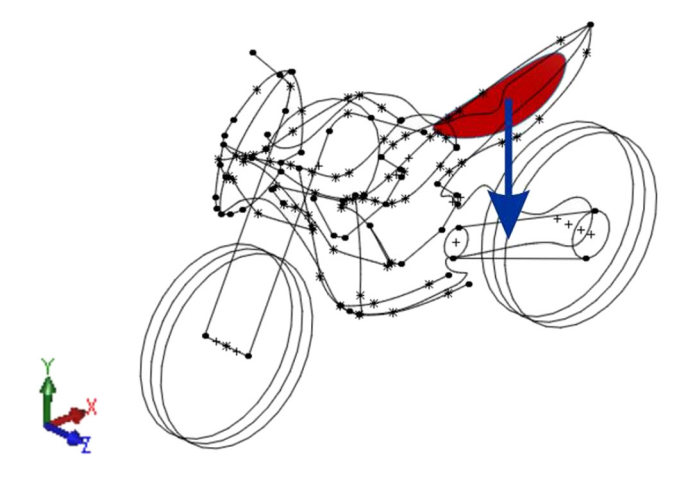


Figure 11: The force of gravity of passengers on a spatial diagram.

of the front fork will allow you to specify the position of the bearings that fix the handlebars to the vehicle frame (Figure 12). The angle between the normal to the contact surface of the wheel with the ground and the axis parallel to the axis of the fork is called the angle of attack. It is one of the variables responsible for the value of the distance referred to as the "mechanical trail," affecting the geometry of the vehicle. The "mechanical trail" is designed to allow greater control of the motorcycle, it also affects the behavior of the vehicle when turning the steering wheel or tilting. This value also affects the behavior when braking with the front brake and the gyroscopic effect produced by the wheels, which in turn allows the vehicle to stay vertical [8] (Figure 12).

Most motorcycles produced on the market have an angle of inclination with values in the range of 23°–30°, of which 27° is considered the "magic value" [8] (Figure 13). Based on this knowledge and due to the generally assumed

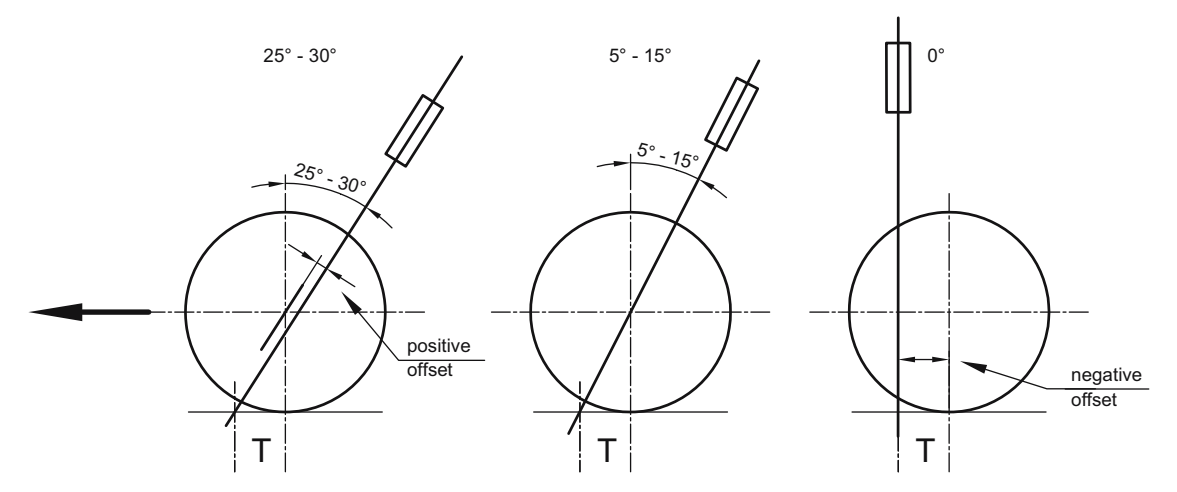


Figure 12: Geometry of the angle of attack of the front fork (own study based on [8]).

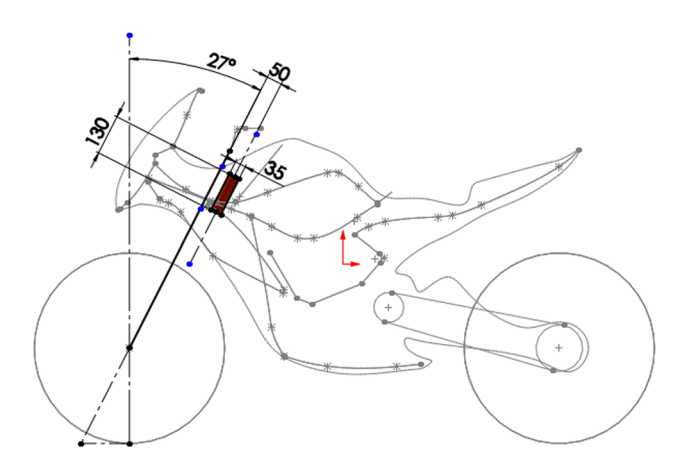


Figure 13: The angle of inclination and the mounting surface of the steering wheel bearings.

dimensions of the vehicle, the above angle was selected for the construction of the designed motorcycle (Figure 13). Then, changes were made to the scheme and the mounting surface of the bearings was determined.

The rear suspension includes a fork or forks, shock absorbers, chains and various types of fastening, and stress transfer structures. There are many types of rear suspension, differing in the number of shock absorbers, wishbones, their position, shape, and mechanically interacting elements.

In the project discussed in this work, a construction based on a combination of one shock absorber and a two-arm fork made of aluminum alloy was used. A chain drive was also used. The frame structure needs to be reinforced in the area where the rear fork and shock absorber are mounted, due to the relationship between the forces acting on the wheel and the shock absorber.

This dependence applies to the forces during the "folding" of the suspension: the wheel moving along the vertical axis transfers the force to the shock absorber, as the difference between the distance covered by the wheel and the distance covered by the shock absorber attachment point increases, the force acting on this point increases. This increase is the square of the ratio of roads covered [8] (Figure 14). The load on the wheel (F) is half the load on the spring (2F), but the vertical movement on the wheel (A) will be twice that of the spring (B). In simple terms, this means that the smaller the stroke of the shock absorber compared to the stroke of the rear wheel, the greater the forces acting on it, which means an increase in the stress on the shock absorber attached to the frame. Therefore, this area of the structure must be reinforced.

Bearing this dependence in mind, the mounting positions of the shock absorber and the rear fork were determined in the spatial scheme so as to obtain the most

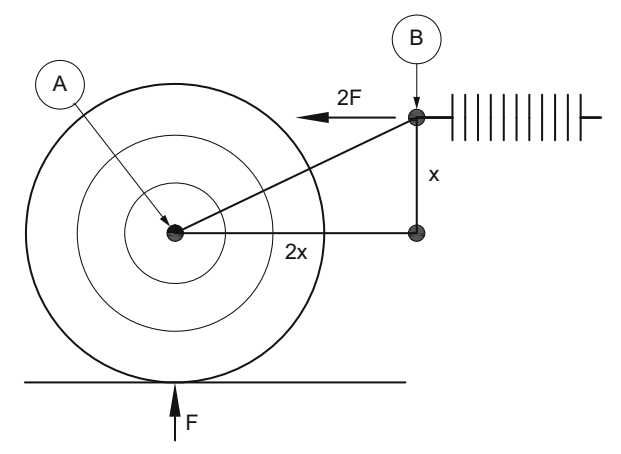


Figure 14: Typical 2:1 leverage system (own study based on [8]).

favorable arrangement of elements in terms of weight and strength (Figure 15).

Based on the above sketch, the component mounting surfaces were created as part of the frame geometry guidelines.

As the last assumption, the type of frame structure was defined. The simplest division of the types of construction of motorcycle frames in terms of production is the division into frames: welded from semi-finished products, welded from elements after plastic processing and from cast elements. For the designed vehicle, a tubular and skeletal structure was assumed, made of welded aluminum pipes made of AlZnMg - 7050-T735 material. It should be noted that at the same time it will also be a structure in which the drive unit designed above will be a structural part, partially responsible for the rigidity of the structure. In the area of engine mounting, a semi-finished product made using additive manufacturing technologies will be attached to the structure.

After determining all the assumptions for the frame construction, a spatial diagram of the structure was

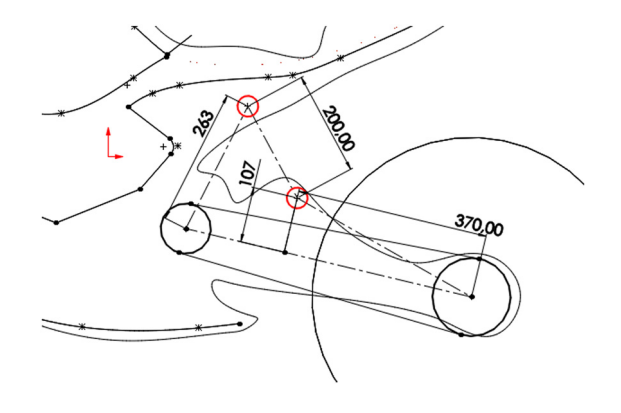


Figure 15: Flat diagram of the shock absorber position.

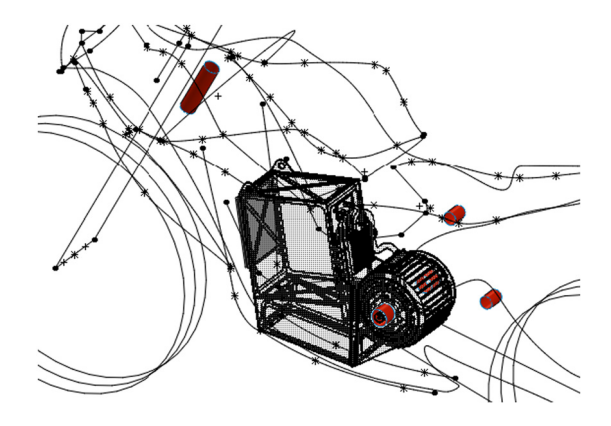


Figure 16: Spatial diagram of rear suspension mounting.

obtained, imposing some dimensions (Figures 16 and 17). On its basis, the construction of the frame will be made.

Once the part is ready, the modeling process can begin. It was started with the projection of the connection surfaces and the creation of appropriate solids on their basis (Figure 18).

On the basis of the obtained geometry, guiding curves were created in accordance with the generally accepted design assumptions. For this purpose, the axes of the resulting cylinders were created and, using the 3D Sketch tool in the SOLIDWORKS 2019 application [6], lines and curves corresponding to the axes of aluminum tubes were determined. The dimensions of the created solids were also adjusted (Figure 19).

Then, surfaces normal to the axis were created and sketches were drawn in them, reflecting the cross-section of the pipe. During the design work, defined global variables were used to determine pipe diameters and their thickness. Global variables for the designed frame were determined based on tables of normal dimensions and catalogs of standardized semi-finished products. In the



Figure 18: Solids of the mounting frame of the vehicle subassembly.

next step, using the sweep operation, the body of the wrought pipe, which is part of the structure, was created (Figure 20).

The operation was repeated for all the curves on one side, and then the mirror operation was used, achieving the initial geometry of the frame. The distances from the elements of the scheme were checked and the dimensions

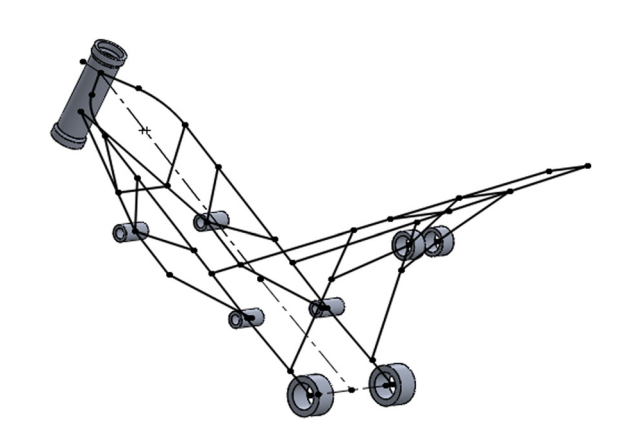


Figure 19: The 3D sketch of the frame structure.

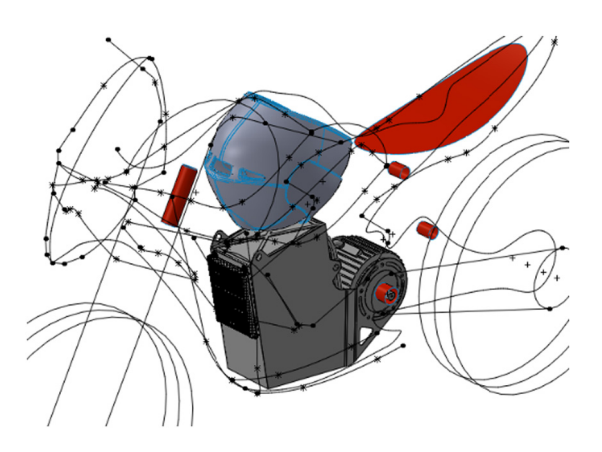


Figure 17: Spatial diagram of the vehicle with spatial guidelines.

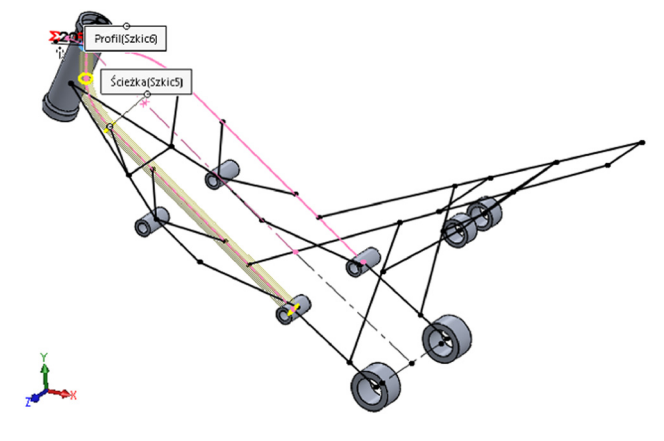


Figure 20: Sweeping a structure element in SolidWorks application.

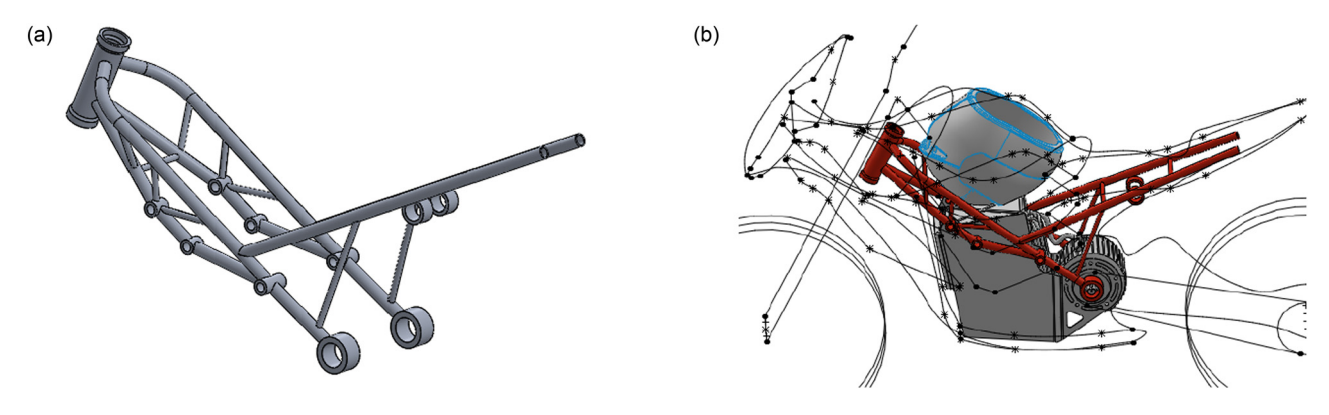


Figure 21: (a) Frame model after initial operations and (b) model of the frame after the initial operations inside the diagram, along with the indicated position of the drive system.

of the openings were refined. Due to the formation of undesirable geometry inside the holes and pipes, it was removed using the extruded cut and extruded cut along the path (Figure 21).

After checking the correctness of the geometry, changes were made to the structure, shock absorber mountings and angles stiffening the structure were added, and several structural changes were made (Figure 22). After these operations, the model was divided into three parts: the main part of the frame and two rear suspension arm mounts, in order to perform a topology analysis of these elements. The resulting models were connected by bonds (Figure 22). The prepared model was then simulated using the FEM.

As shown in Figure 22, the entire motorcycle frame consists of a welded structure of aluminum tubes marked as (1) and an additional element marked as (2). Element (2) connects the proper part of the frame, supports the engine and is the place where the rear swingarm is attached. Due to the rather complex shape, in the discussed project it was decided to make this element using additive manufacturing techniques, through 3D printing from metal powders. This

will allow us to obtain a shape unattainable by other production methods

3.2 Simulation tests of the frame support element – an element produced by incremental methods

The strength of the frame connectors can be assessed in several ways. The first one is standard analytical calculations, based on commonly known formulas, tables, and strength graphs [11–13]. The second option is to make a prototype and subject it to strength tests. The third possibility is comprehensive simulation research, conducted on virtual models, using CAE tools. Among the simulation studies, the FEM [7], widely used in engineering, should be mentioned, which is often extended by topology research, referred to in many sources as topological optimization. Topological optimization is also very often used in the process of designing structural elements produced by

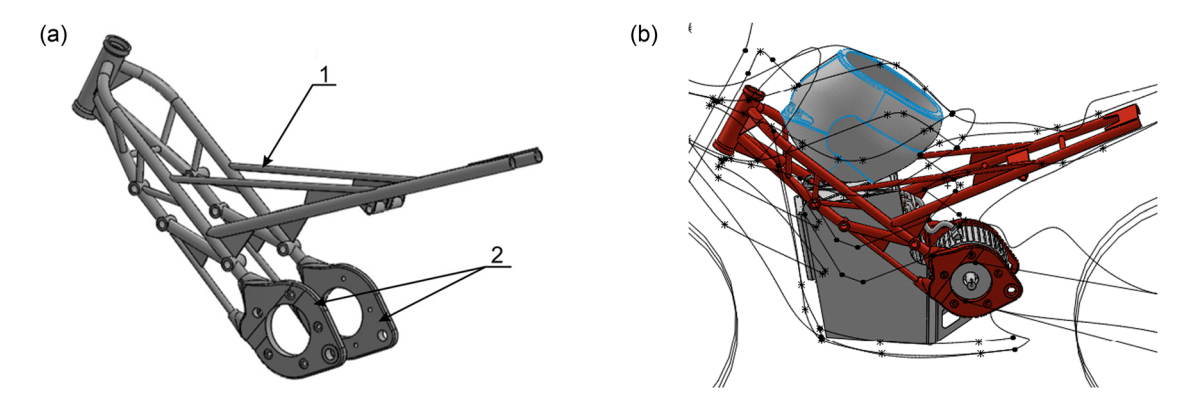


Figure 22: (a) Modified frame model and (b) frame model after initial modifications inside the diagram.

incremental methods, e.g., during the metal powder printing process. This production process makes it possible to obtain shapes that are difficult to achieve by conventional manufacturing methods. Based on the results of the simulation study, which is topological optimization, a geometry with better mechanical properties is generally created.

Topological optimization [6] consists in finding a geometry that meets specific and well-defined strength requirements, based on the original shape of the element. It is generally used to reduce weight, determine the best stiffness-to-weight ratio, or minimize displacements of a structure subjected to loads. During the design process, based on topological optimization, on the basis of the solid obtained from the simulation test, the tested element is adapted to its results, working out a compromise between technological possibilities and optimal geometry [6]. Among the many publications in which attention is paid to the issues of topological optimization, one can refer to [14–18,20].

In the design of the described motorcycle, it was assumed that one of the parts of the frame, fixing the engine, would be manufactured using unconventional production methods – additive methods, allowing the creation of complex geometry in all axes of the coordinate system. Therefore, the only geometric assumptions during the FEM simulation study and topological optimization will be the behavior of the solids surrounding the areas of contact with other elements and the minimum thickness of the geometry.

The tested element – presented in Figure 23, is a structural part of the vehicle frame, it fastens the frame skeleton to the drive unit, while being the point of attachment of the rear swingarm. The block has holes for M8 screw connections with the assembly and the motor. The part also connects two pipes that are part of the skeleton. The applied connection fixes the ends of the pipes inside the openings, enabling bolt or weld connection. In Figure 23, the connection surfaces are marked in red.

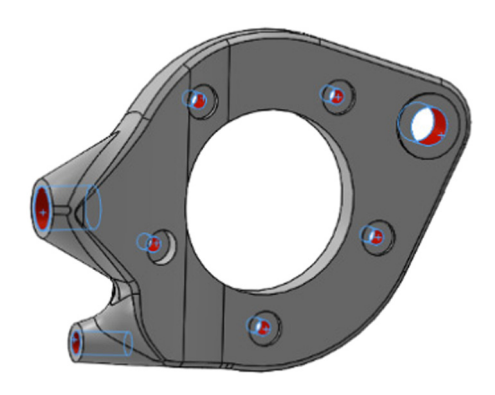


Figure 23: Connection surfaces of the tested element.

The initial mass of the element, estimated using the CAD module of the SOLIDWORKS 2019 application [6], is approximately 1,110 g, using the material of the 7050-T7351 aluminum alloy for the model. The 7,000 series aluminum alloy is an elastic-plastic material, one of the materials used in additive manufacturing. It should be emphasized that the purpose of the study is mainly to increase strength, taking into account the low mass of the original element.

Conducting simulation tests requires proper definition of the forces acting on the frame and its components. The forces acting on the elements will be distributed evenly on both fasteners. The distribution of static forces acting on the elements was assumed as 50% of the weight of the drive unit (denoted as $m_{
m drive_unit}$), 60% of the weight of the frame skeleton (denoted as $m_{\rm skeleton_frame}$), and 100% of the weight of the mass associated with the users (denoted as $m_{\rm users}$), and 50% of the assumed weight of the remaining vehicle elements, amounting to about 40 kg, was added to these values (denoted as m_{other_items}). The obtained value was divided by two in order to obtain the force acting on a single element - there are two symmetrically located tested elements in the frame. It should be noted that dynamic forces related to the movement of the vehicle or the operation of the rear suspension of the vehicle were not assumed. Therefore, the geometry adjustment process will assume a thicker solid on the axes between fixtures. The mounting surface of the swingarm was assumed to be stationary. The distribution of forces was assumed to be 90% of the value for the mounting elements with the frame and 10% of the value for the holes for screw connections.

Using the SOLIDWORKS 2019 application [6], the weight of the frame skeleton was estimated at 2.02 kg (Figure 24).

Then, the mass of the system acting on both connectors was calculated in accordance with the previous paragraph. The calculations were carried out assuming the acceleration due to gravity, $g = 9.81 \,\mathrm{N/kg}$, and the obtained value was divided by two.

$$m_{\text{system}} = 50\% \cdot m_{\text{drive_unit}} + 60\% \cdot m_{\text{skeleton_frame}} + m_{\text{users}} + 50\% \cdot m_{\text{other items}},$$
 (5)

$$m_{\text{system}} = 50\%.53 \text{ kg} + 60\%.2.02 \text{ kg} + 200 \text{ kg} + 50\%.40 \text{ kg} = 247.712 \text{ kg},$$
 (6)

$$Q_{\text{system}} = 247.712 \text{ kg} \cdot 9.81 \frac{\text{N}}{\text{kg}} \approx 2,430 \text{N},$$
 (7)

$$Q_{\text{one_element}} = 2,430\text{N} \cdot \frac{1}{2} \approx 1,215\text{N}.$$
 (8)

As can be seen, the load on the motor mount is equal to 1,215 N.

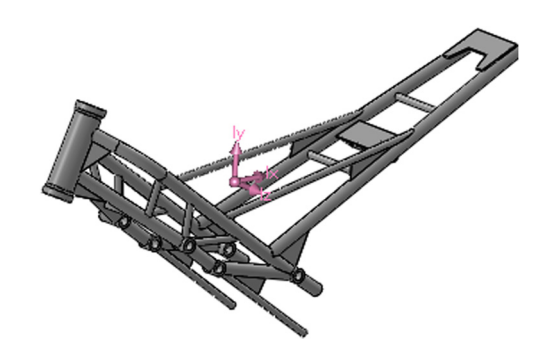


Figure 24: Skeletal shape of the frame, without rear swingarm mounts.

Simulation studies began with the analysis of the original geometry with assumed loads. In order for mass to be removed from an element, it must initially meet the strength requirements. A safety factor of k=3 was assumed for the structure, which for the material used means reference stresses of $\sigma_{\rm ref}=145$ MPa [12,13].

$$\sigma_{\text{ref}} = R_{\text{e}} \cdot \frac{1}{k} = 435 \text{ MPa} \cdot \frac{1}{3} = 145 \text{ MPa}.$$
 (9)

In the next step, a static analysis was performed in the SOLIDWORKS 2019 application [6], using the SIMULATIONS add-in. On the developed model of the element, the assumed loads were imposed, the surface of the rocker arm mounting hole was immobilized and a finite element mesh was created. To fill the mesh, tetrahedral solid elements of the SOLID type, of high quality, were adopted. This means that it is a second-degree element [6], with ten nodes four at the vertices (corners) and six at the midpoints of the edges. The selection of the second-degree element, not the first one, which is an element of draft quality (a tetrahedron with four nodes in the corners), allows for a better representation of the curvature before and after deformation as a result of acting external loads. The high-quality finite elements with ten nodes assumed in the model represent the displacement field in the form of a parabolic

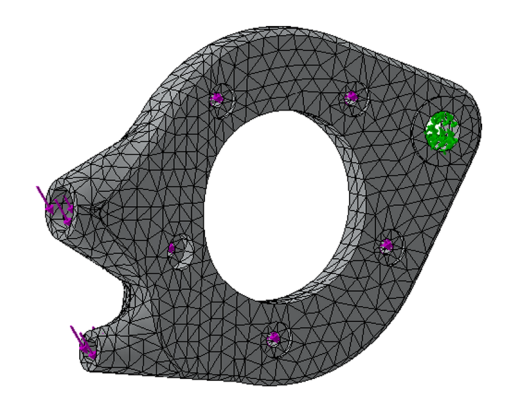


Figure 26: Grid of the static analysis of the tested element.

function. As a consequence, the stress and strain fields are approximated in a linear way. In order to obtain reliable results, in the model under consideration, according to the suggestions of the authors of the SOLIDWORKS 2019 application [6], at least two elements were used in the thickness of the model. The finite elements adopted for filling in the model had four Gaussian points each, which means four points of numerical integration in the element. The numerical model of the considered element consisted of 11.169 finite elements (the total number of nodes was 18,031), with an average element size of 8.6 mm. Figure 25 shows the model of the tested element with applied forces (purple arrows) and fastening as stationary geometry (green arrows). Figure 26, on the other hand, shows the discretized model of the tested element, including the mounting and the applied load.

Figure 27 presents the distribution of effective stresses calculated according to the Huber-Mises-Hencky (HMH) hypothesis [11–13] for the considered element. The maximum effective stresses in the block are approximately 94 MPa, which means that the element does not deform plastically. This value is about 22% of the yield point σ_0 and 65% of the reference stresses, determined from the

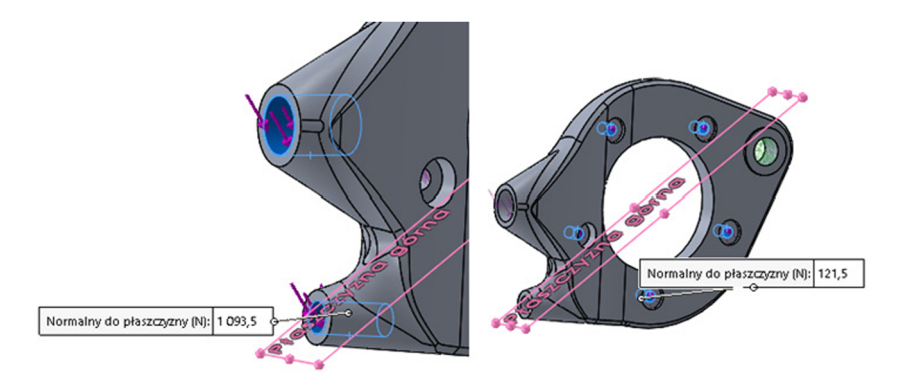


Figure 25: Static forces acting on the tested element.

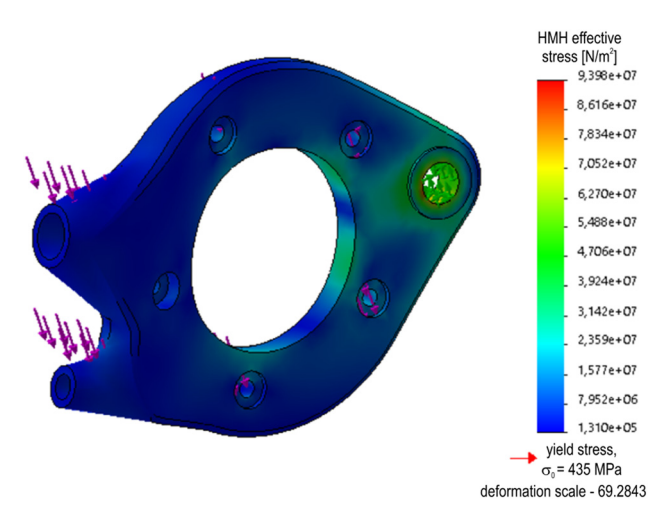


Figure 27: The HMH stress diagram of the static analysis of the tested element.

formula (9). Then, the calculations were repeated for the model with 16 Jacobian points, which did not affect the obtained results. It should be noted that the Jacobian points are points used to check the Jacobian ratio which is a measure of mesh quality. Change from 4 to 16 points does not affect the results in terms of stress, but differently highlights the mesh quality. As can be seen, the greatest stresses radiate from the surface of the rear control arm mounting hole, which requires adjusting the tested element in order to strengthen it. The remaining area of the geometry is generally characterized by relatively low values of effective stresses (Figure 27).

When analyzing the obtained effective stress distributions, the reader may notice that the SOLIDWORKS application [6] displays most of the simulation results using the deformation scale [6]. The deformation scale refers to the scale factor that the program uses to scale the deformed shape of the model. The value of the scale factor depends on the largest dimension of the model and the calculated deformations. For example, a scale factor of 50 means that the largest deformation calculated in the simulation add-in of SOLIDWORKS application [6] is 50% greater than the largest dimension of the smallest bounding box surrounding the model. A larger deformation scale factor improves the visualization of deviations that are much smaller compared to the original dimensions of the model. In the distribution of effective stresses presented in Figure 27, the automatic deformation scale was 69.2843. This means that the actual displacement has been magnified that many times. This procedure is used in order to better present the way the model works [6].

After confirming the strength of the structure, the topology study was started [14–18]. Due to the characteristics

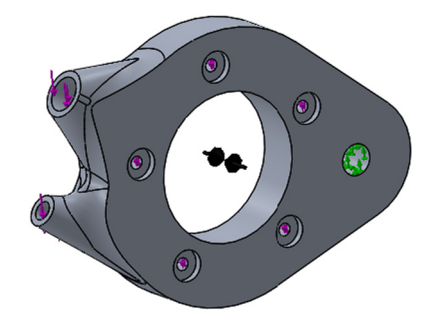


Figure 28: New form of the tested element. Loads (purple arrows) and fastenings (green arrows) in the topology study.

of the process performed by the program, the geometry of the element was slightly simplified, the model was made thicker, and reinforcement was introduced by adding material in the place where the rear swingarm is attached. At this stage of the design, it turned out that the weight of the element increased significantly to 1.9731 kg (Figure 28).

In the improved fastening model, similar to the previous study, during topological optimization (which other researchers used in their works [14–18]), forces were fixed and the model was immobilized (Figure 28). The test objective was defined as "The best stiffness to mass ratio," and then the mass linkage goals were selected as reducing it to 50% of the original mass and linking the maximum stresses with the previously defined value of allowable stresses (assuming that the yield strength of the material is σ_0 = 435 MPa, and allowable stresses $\sigma_{\rm ref}$ = 143.5 MPa – i.e., 33% of the yield strength – this means that the calculations were carried out with the assumption of the safety factor x = 3 [13]).

Before the analysis, it was indicated that the minimum thickness of the member should be 6 mm in each axis. All contact surfaces are marked as areas to keep and are 4 mm thicker. The plane of symmetry and the direction of

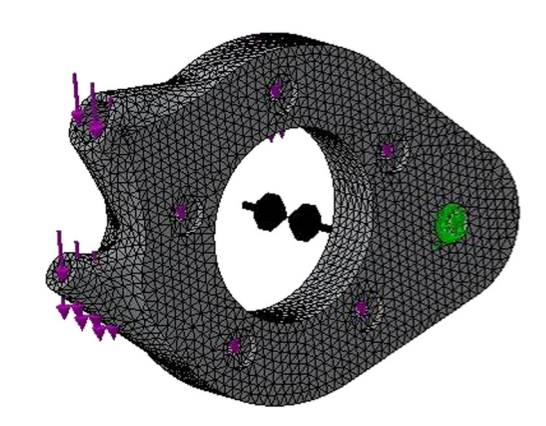


Figure 29: Solid mesh in a topology study.

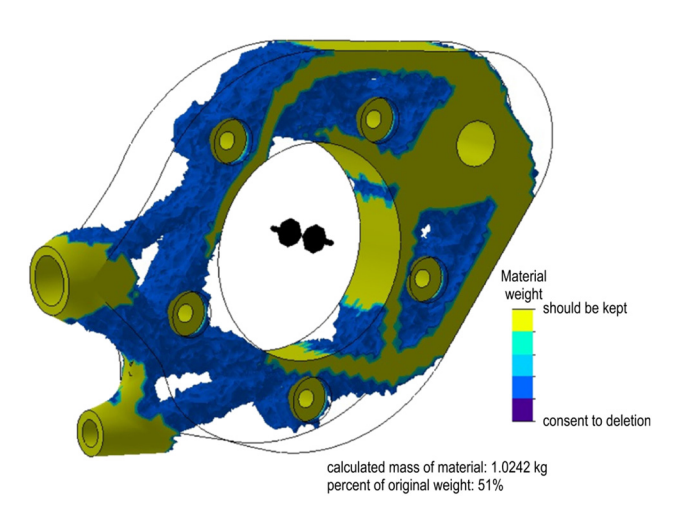


Figure 30: Results of element topology simulation.

molding the solid were not defined due to the assumed production method. After defining all assumptions of the analysis, a finite element mesh was created with four Gaussian points in a high-quality finite element (tetrahedron with ten nodes, as in the study described above), total number of nodes –115,996, total number of finite elements – 78,460, and an average element size of 4.65 mm. Figure 29 shows the FEM model used in the topological optimization simulation.

The study of topological optimization required the application processor to run 36 iterations of the solid geometry. The result of the optimization is shown in Figure 30, which shows the graph of the mass distribution that can be removed. For further analysis, a variant with an element mass of 1.0242 kg was adopted, which means a reduction of almost half the value before the test, similar to the original model, whose mass was 1.9731 kg.

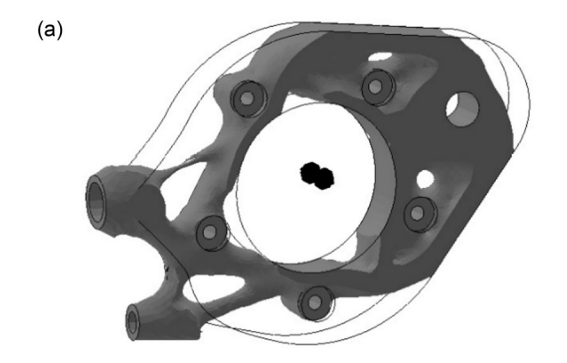
Figure 31a shows the tested element smoothed after the topology test, on the basis of which a new variant of the structure element was developed. Therefore, the obtained

geometry (in the form of a points cloud) was exported to a file with the *.stl extension, and then, when modeling a new part, the obtained geometry was imported to it, and then its transparency was changed. Individual elements of the original part were also projected using the 3D Sketch tool in SOLIDWORKS application [6]. Based on this data, a new part was constructed as shown in Figure 31a.

The next step was to create a new part and import the resulting geometry into it, then change its transparency. Individual elements of the original part were also uploaded in the form of 3D sketches. Based on this data, a new part was created, constructed as shown in Figure 31b.

After the initial model creation, as well as the process of gradual improvement of the geometry in terms of strength, a solid with a mass of 1 kg was obtained, as shown in Figure 32, which was subjected to another FEM simulation, carrying out a static analysis study, based on restraints and common loads with the study of the initial geometry, only changes were made to force distribution of 121.5 N, adding two additional surfaces of its impact, which are the bearings of the motor shaft. In the model, a mesh of tetrahedral ten nodal finite elements with four Gaussian points in the element – solid elements of high quality – was created. The generated mesh consisted of 38,914 finite elements (i.e., 66,109 nodes) with an average element size of 4.95 mm.

The results of the simulation are shown in Figure 33. In the tested element, the estimated maximum effective stresses calculated according to the HMH hypothesis [11–13], with the assumed loads and fastenings, are approximately 32 MPa, which means a value nearly three times lower compared to the model test (i.e., 94 MPa), and at the same time more than four times lower than the accepted allowable stress (i.e., 143 MPa). As can be seen, the effective stresses are more evenly distributed in the solid, which results in a prolonged process of material degradation. It should be noted that the production method used (incremental method – 3D printing from metal powders) may reduce the mechanical properties



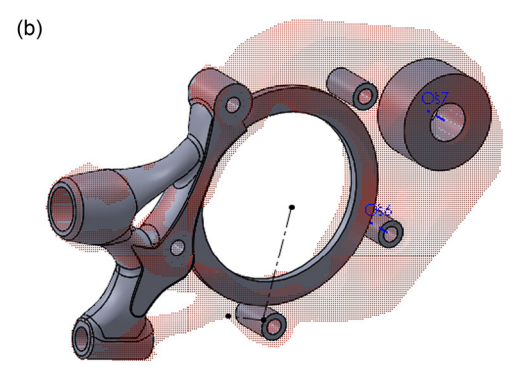


Figure 31: (a) Smoothed element mesh and (b) the process of modeling a new solid of the tested element.

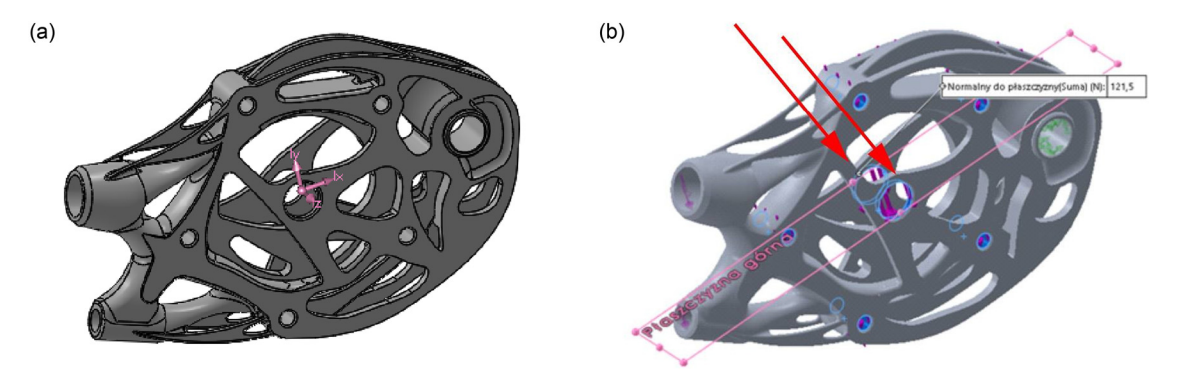


Figure 32: Additional load mounting surfaces.

of the material, but due to the achievement of stresses more than ten times lower than the yield strength of the selected material (435 MPa), this issue can be omitted. The numerically estimated displacements in the solid reach a maximum value of 0.15 mm (Figure 34).

The weight of the modified component is 1.001 kg, which means a decrease in weight of 109 g compared to the initial value (1.110 kg). The resulting mass of the element can also be reduced by using an appropriate structure instead of full filling inside the geometry, which may be the subject of other considerations or a research project in the future. Comparing the original element and the element obtained on the basis of topological optimization (Figure 35), it can be seen that the general profile of the element has been preserved, changing only its width in the places where the bolts and the rear wishbone are attached. A hoop supporting the motor shaft has also been added (Figure 35). Figure 36 shows the entire vehicle frame, including the element obtained as a result of topological optimization.

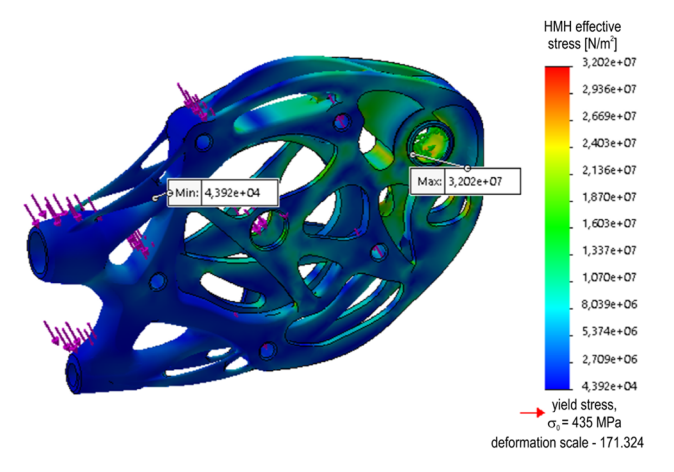


Figure 33: The distribution of the HMH effective stress in the modified solid.

3.3 Simulation tests of the frame support element – an element manufactured by an alternative method

On the basis of the geometry developed in the topological optimization, an alternative version of the element connecting the main frame and the rear swingarm was developed, which can be produced in the casting process (Figure 37). The demolding direction parallel to the axis of the M8 holes was determined (blue arrows in Figure 37), and then the geometry was created in accordance with the technological possibilities. The element was adapted to create a casting mold, and then to make holes impossible to be included in the form by drilling – red arrows in Figure 37. The weight of the estimated solid is about 1 kg.

The obtained geometry was subjected to static analysis, assuming loads and restraints in accordance with the previous test. A mesh of ten nodal tetrahedral finite elements was created with four Gaussian points in an element, total number of nodes of 76,406, total number of elements of 37,823, and an average element size of 6.27 mm. The numerically determined effective stresses, calculated according to

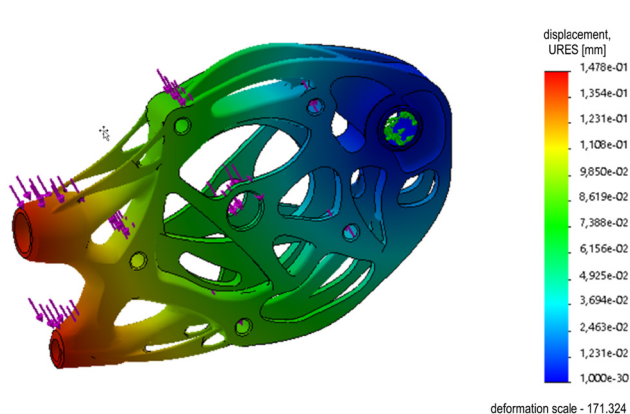


Figure 34: The distribution of the displacement in the modified solid.

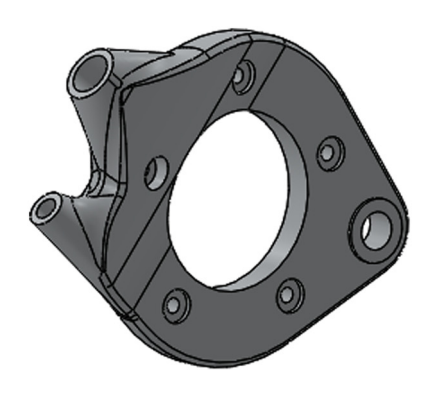




Figure 35: Visual comparison of the mounting bodies.

the HMH hypothesis, do not exceed the value of 25 MPa, which is a value 7 MPa lower than in the study of the solid intended for production by incremental techniques (Figure 38). The estimated stress distribution is characterized by less dispersion compared to the previous variation. Displacements also slightly decreased (Figure 39). The obtained results allow to conclude that the structure meets the requirements set out at the beginning. It should be noted, however, that despite the better mechanical properties of the alternative element (manufactured by casting), it may turn out to be problematic in the technological process and may be characterized by lower stiffness under the influence of torsional forces.

3.4 Analysis of the structure of the proper frame using the FEM

The next step in the frame design process is to check its stiffness and eliminate areas of high stress by analyzing the geometry using the FEM. For this purpose, two simulation tests were carried out: a static simulation of the frame under full load and a frame test under the force acting on the frame in the process of rapid braking.

3.4.1 Full load frame test - FEM analysis

Simulation studies, as before, were performed using the SIMULATIONS add-in in the SOLIDWORKS 2019 application [6]. The imported frame had to be properly fixed and loaded. The boundary condition of the fixed geometry was assumed as the front fork and rear swingarm mounts (Figure 40). In the next steps, the structure had to be properly loaded, taking into account all components derived from the weight of the drive unit, the weight of the driver and passenger, the weight of the bodywork and other components of the motorcycle structure, and the reaction force of the suspension acting on the shock absorber mounting (Figures 41–43).

The load from the drive unit was divided into two different parts. It was assumed that the frame elements are affected by 75% of the weight of the drive unit on the



Figure 36: The vehicle frame after the use of modified solids.

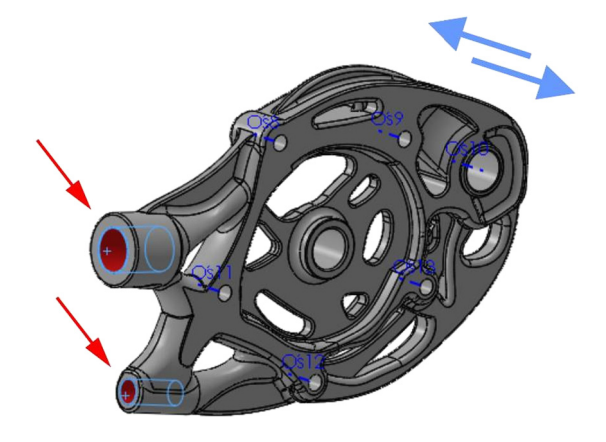


Figure 37: Alternative solid with marked drilling surfaces and demolding direction.

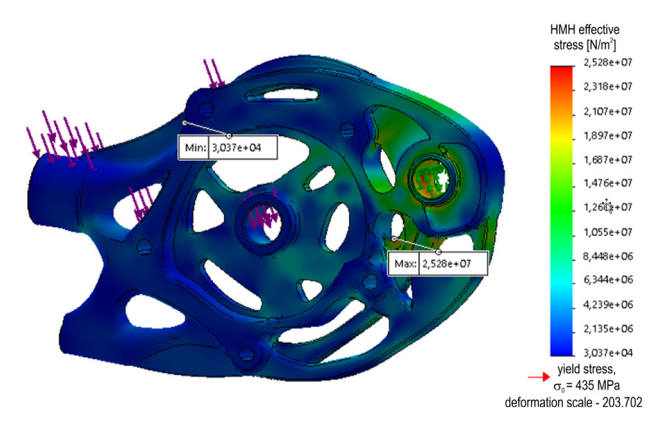


Figure 38: The distribution of the HMH effective stresses in an alternative solid.

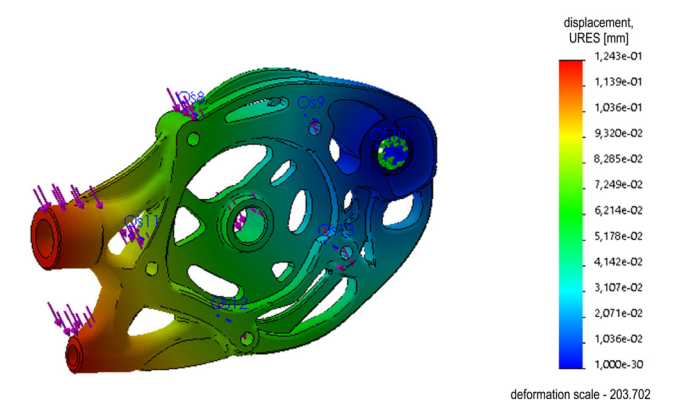


Figure 39: Distribution of the calculated displacements in an alternative solid.

M15 screw holes (Figure 41a) and 25% of the weight of the drive unit on the holes of the M8 screw connections inside the connector bodies (Figure 41b). The applied forces have been rounded to units.

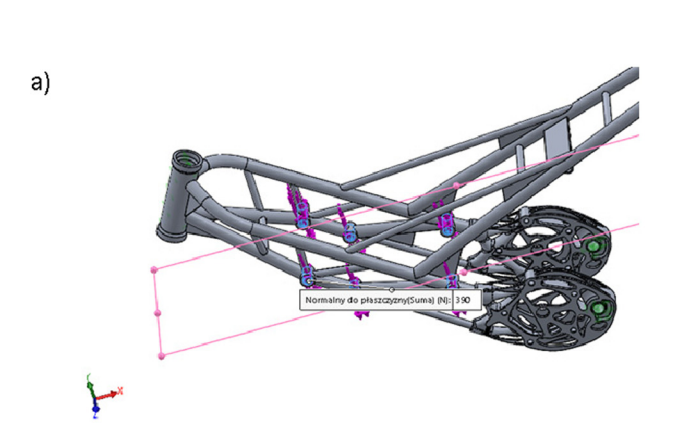


Figure 41: (a) Load Q_1 in a static load test and (b) load Q_2 in a static load test.

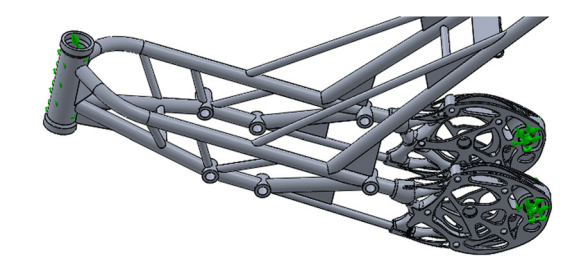


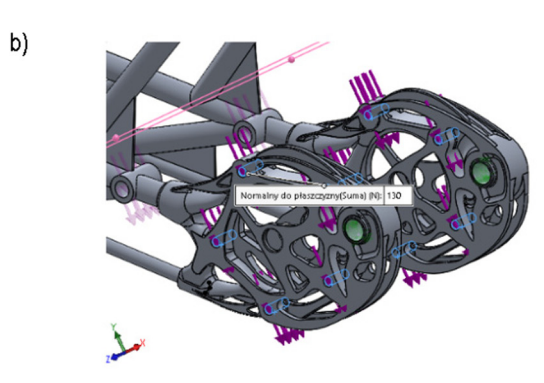
Figure 40: Fixed geometry in a static load study (boundary conditions are marked using green arrows).

$$Q_{\text{drive_unit}} = 53 \text{ kg} \cdot 9.81 \frac{\text{N}}{\text{kg}} = 519.93 \text{N}$$

 $Q_1 = 519.93 \text{N} \cdot 75\% = 389.9475 \text{N} \approx 390 \text{N}$
 $Q_2 = 519.93 \text{N} \cdot 25\% = 129.9825 \text{N} \approx 130 \text{N}$. (10)

The load of the driver and passenger with the value $Q_3 = 2,000$ N was imposed on the frame in the designated area of the seat attachment (Figure 42a). The load on the car body and other elements was assumed as $Q_4 = 300$ N. The model was divided and the force was fixed on an exemplary surface transferring the load (Figure 42b). The suspension reaction force acting on the shock absorber mounting was assumed as $F_1 = 500$ N. The force vector was drawn along the assumed shock absorber axis (Figure 43).

After mounting the entire frame and imposing forces on the system, the model was discretized. A mesh of tetrahedral ten nodal finite elements with four Gaussian points in the element was created. The total number of elements in the model was 101,840, and the number of nodes was 198,953. The model used grid control for selected areas, changing the size of the finite element in the range of 6.21–30.61 mm. The material of the elements has not been changed. Figure 44 shows the discretized model of the frame with the rocker arm connector intended for production by 3D printing, along with the assumed boundary



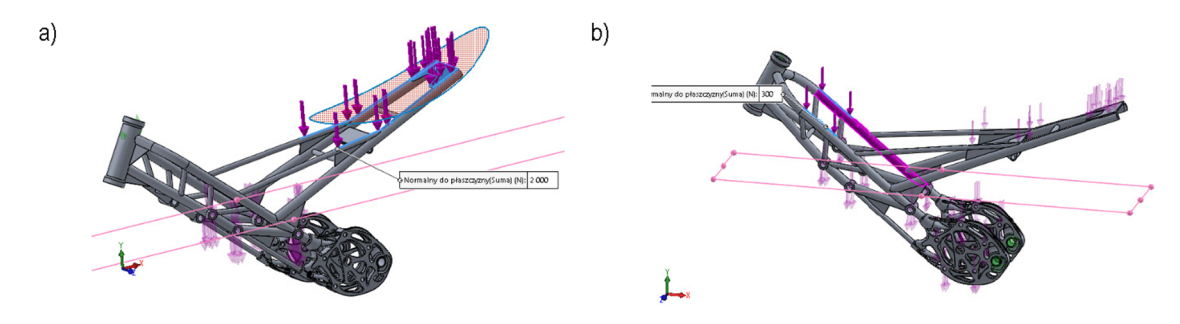


Figure 42: (a) Load Q_3 in the static load test and (b) load Q_4 in the static load test.

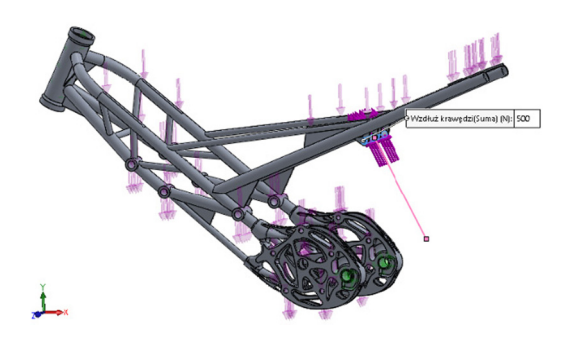


Figure 43: Force F_1 in a static load test.

conditions – fixed mounting (green arrows) and applied load (purple arrows).

The performed simulation shows that for the given boundary conditions and load, the effective stresses calculated according to the HMH hypothesis are lower than the assumed yield point, but relatively high – in some places they exceed 350 MPa – so they are more than 2.5 times higher than the allowable stresses determined by the formula (9) – $\sigma_{\rm ref}$ = 143 MPa. Figure 45 shows the places where the stresses are greatest. Estimated results indicate the need to strengthen the

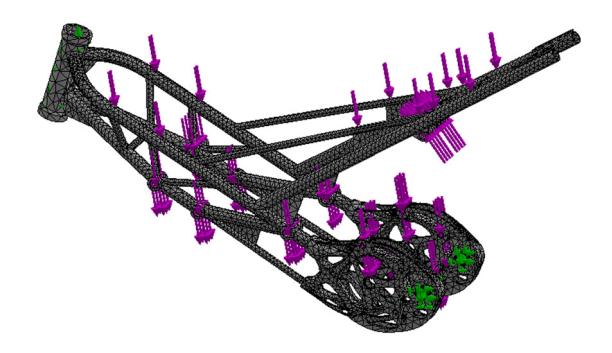


Figure 44: Mesh of the whole frame of the electric motorcycle, used in a static load test.

structure. The occurrence of maximum effective stresses in the shown place results from the fact that the structure does not contain pillars supporting the frame in the resting place of the driver and passenger, which results from the adopted style of the vehicle body to make it visually attractive, in accordance with the design principles.

In order to eliminate the value of effective stresses in the frame structure, it was strengthened by using additional elements produced by plastic working methods

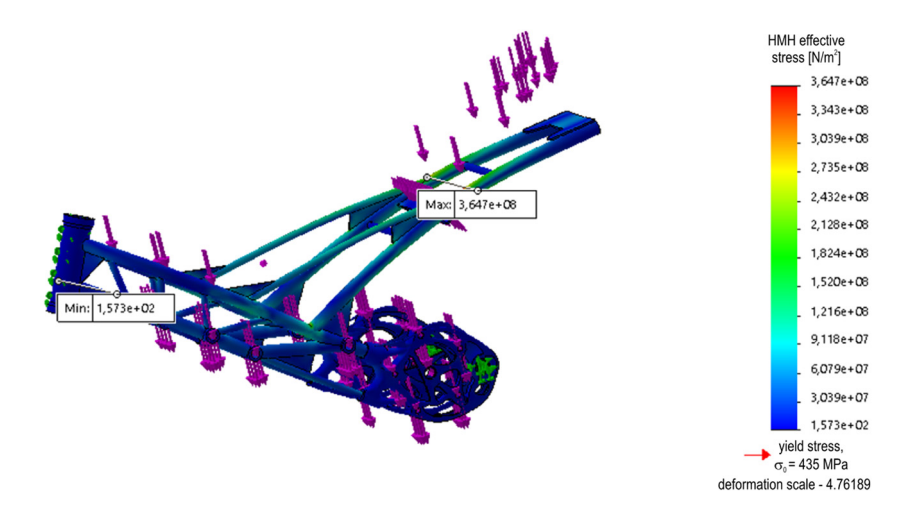


Figure 45: The distribution of the HMH effective stress, calculated in a static load test.

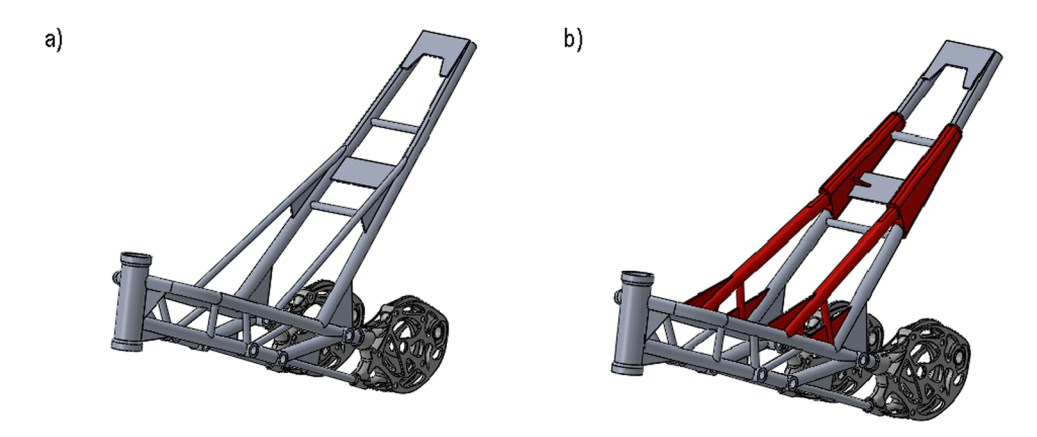


Figure 46: Structure - full frame of electric motorcycle before (a) and after (b) modifications in the static load test.

and by casting. Angles under the seat were abandoned and angles were added in areas of high stress, and the pipes connecting the seat were thickened. A comparison of both frame models is shown in Figure 46. Changes introduced to the frame structure are marked in red in Figure 46b.

In the corrected version of the frame, fixed attachments were added as before and the abovementioned loads were applied (Figure 47). The virtual model was discretized by filling up to tetrahedral SOLID finite elements with ten nodes and four points of numerical integration. As before, in selected areas of the structure, mesh control was applied by changing the size of the finite element, in the range of 6.5–30.06 mm. The entire frame model was filled with 112,362 finite elements. The total number of nodes in the model was 207,211. The estimated effective stress in the entire model turned out to be lower than the value of allowable stress determined by the formula (9) ($\sigma_{\rm ref}$ = 143 MPa). The maximum value of effective stresses is 76% of allowable stresses. The simulation carried out indicates

an even distribution of stress in the considered structure, in relation to the applied boundary conditions and load (Figure 47).

As shown in Figure 48, the frame moves – flexes up to 6 mm. This deflection was recorded at the end of the seat mounting bracket. It may seem that this is a significant value, but it does not threaten the structure. The estimated amount of deflection is due to the large moment generated by the mass of the passenger. Taking into account the frequency of such a situation, driving with a passenger, which can happen quite rarely, the estimated result can be considered acceptable (Figure 48).

Figure 49 shows the numerically estimated deformations (strains) in the frame structure. As can be seen, their highest value appears in places where the effective stresses were the highest, which is a completely natural and unquestionably acceptable phenomenon. It is worth noting that the maximum deformation value does not exceed 0.13%, which is an acceptable result.

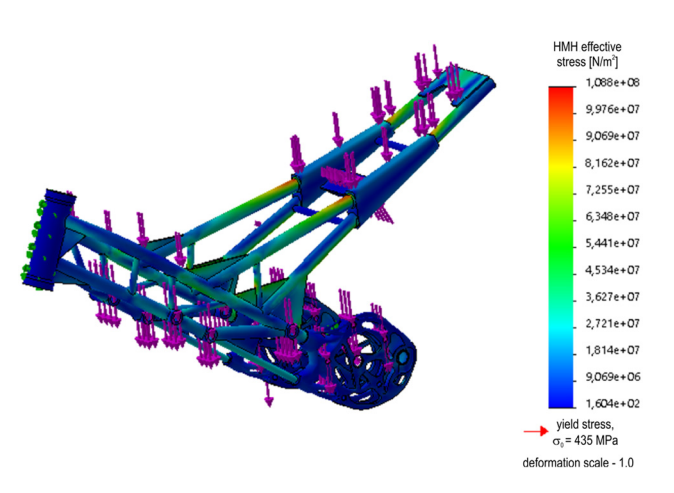


Figure 47: The distribution of the HMH effective stress, estimated in the static load test after modifications.

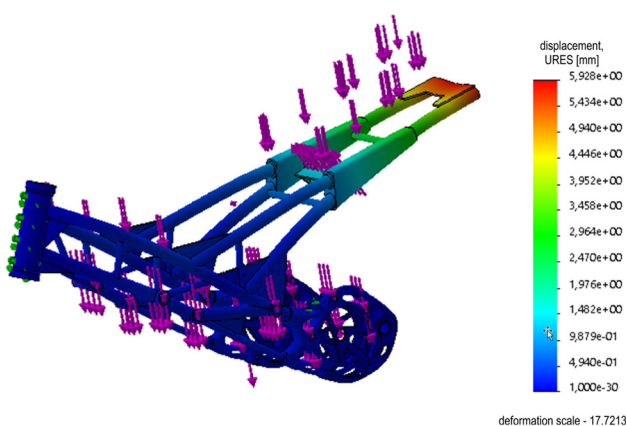


Figure 48: The Displacements distribution, calculated in the static load test after modifications of the frame.

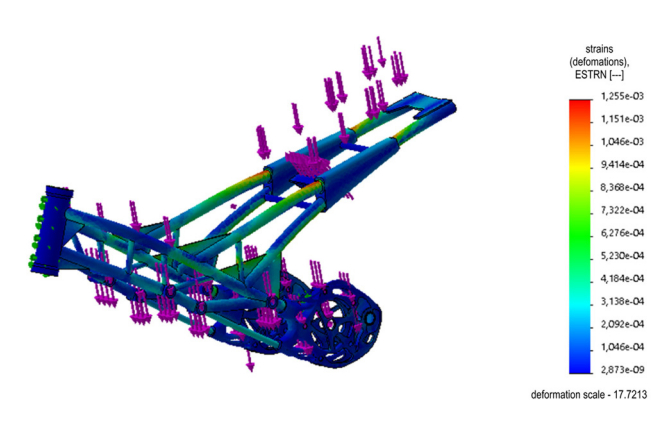


Figure 49: Distribution of the deformations (strains) in the static load test after modifications of the frame.

3.4.2 Testing the frame under the braking force of the system

An important element when riding a motorcycle is the braking situation – the situation of a sudden slowdown of the vehicle. To determine the level of deformation and stress in the frame in such a situation, it was decided to run a simulation when the driver uses only the front brake. In order to carry out the numerical estimation, the initial velocity of the vehicle was assumed, $v_0 = 50 \text{ km/h} = 14.(8) \text{ m/s} \approx 15 \text{ m/s}$, final velocity of the vehicle $v_1 = 0 \text{ km/h} = 0 \text{ m/s}$, braking time t = 4 s, mass of the system (motorcycle and rider): m = 230 kg. To calculate the force F, the following work formula W [19] is transformed:

$$W = F \cdot s \to F = \frac{W}{s},\tag{11}$$

where W is the work, F is the force, and s is the distance. The energy of the system can be determined from the kinetic energy formula [19] as follows:

$$E_{\rm k} = \frac{1}{2} {\rm mV}^2 = \frac{1}{2} \cdot 230 \text{ kg} \cdot \left[15 \frac{{\rm m}}{{\rm s}} \right]^2 = 59,625 \text{J}.$$
 (12)

Then, the required delay is evaluated by

$$a = \frac{V}{t} = \frac{15 \text{ m/s}}{4\text{s}} = 3.75 \frac{\text{m}}{\text{s}^2}.$$
 (13)

Using the formula for the distance in uniform decelerated motion, the braking distance of the system can be calculated [19] as follows:

$$s = v_0 t - \frac{at^2}{2} = 15.4 - \frac{3.75.4^2}{2} = 30(\text{m}).$$
 (14)

Therefore, the forces acting on the system during braking are

$$F = \frac{W}{s} = \frac{59,625J}{30m} = 1987.5N.$$
 (15)

It should be noted that the calculations omitted the friction force, air resistance, spring action of the front suspension, reducing the force acting on the frame, assuming the ideal stiffness of the component. For this reason, it was assumed that the value of 143 MPa could be exceeded by 10%, which means the maximum allowable stress is 157.3 MPa. As a result of elementary calculations, a static force of $F = 1987.5 \,\mathrm{N}$ was obtained, acting on the front fork mounting in the opposite direction to the velocity vector. In order to simulate the behavior of the frame in the described situation, a designated force was applied to the mounting surface of the steering wheel bearings and the load resulting from the mass of the driver and passenger was reduced to Q_5 = 1,000 N. The force area was also reduced, assuming only the mass of the driver. The reaction force of the suspension was also reduced to 250 N. The remaining loads were left. The immobilization of the front fork mount has been removed. The frame model with applied boundary conditions (green arrows) and with applied load (purple arrows) is shown in Figure 50.

The virtual model was discretized by filling up to tetrahedral SOLID finite elements with ten nodes and four points of numerical integration. As before, in selected areas of the structure, mesh control was applied by changing the size of the finite element, in the range of 6.5–30.06 mm. The entire frame model was filled with 112,362 finite elements. The total number of nodes in the model was 207,211. As a result of the numerical calculations (Figure 51), the maximum effective stresses calculated according to the HMH hypothesis in the frame structure slightly exceed the value of 177 MPa. This is an excess of the allowable stresses determined by formula (9). In this regard, it is necessary to strengthen the structure.

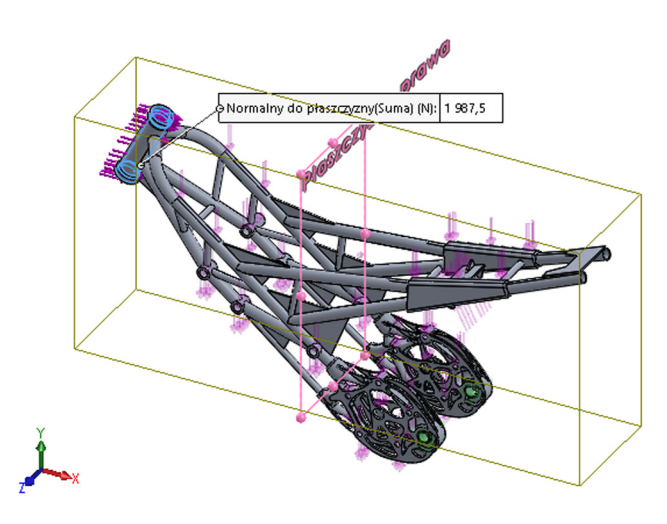


Figure 50: Braking force in a static braking test.

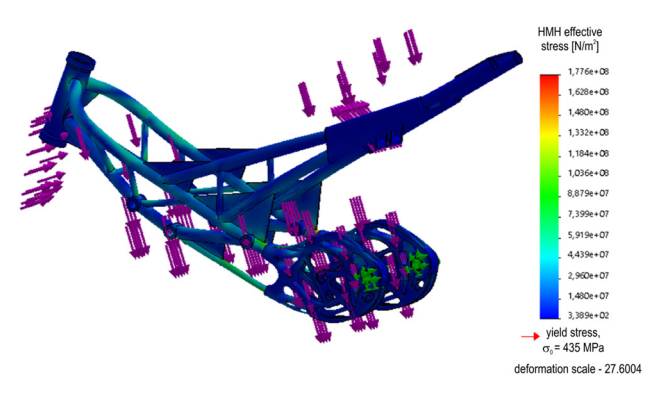


Figure 51: The HMH effective stress distribution, calculated in a static braking test for frame of the electric motorcycle.

Due to the fact that the effective stresses were exceeded by almost 25% of the reference stresses, areas characterized by high stresses in the previous simulation were added by adding pipes supporting the seat support and the adjacent angle bars were thickened. Figure 52 shows the reinforced frame.

The reinforced model of the frame was divided into tetrahedral ten-node finite elements with four Gaussian points in the element. As in the case of previous simulations, the control of the size of elements in the range of 6.05-30.29 mm was used. The total number of nodes that make up the model is 208,292, i.e., 113,153 SOLID finite elements. The fixation and loading of the frame were adopted from the previous simulation. Estimated effective stresses (Figure 53) at two points do not exceed 150 MPa. This value is 7 MPa higher than the permissible stresses determined by formula (9), i.e., 143 MPa; however, at the beginning of the analysis, it was indicated that the calculations omitted the friction force, air resistance, and elastic action of the front suspension, reducing the force acting on the frame, assuming an ideal component stiffness. For this reason, it was assumed that the value of 143 MPa could be exceeded by 10%, which means the maximum allowable stress is

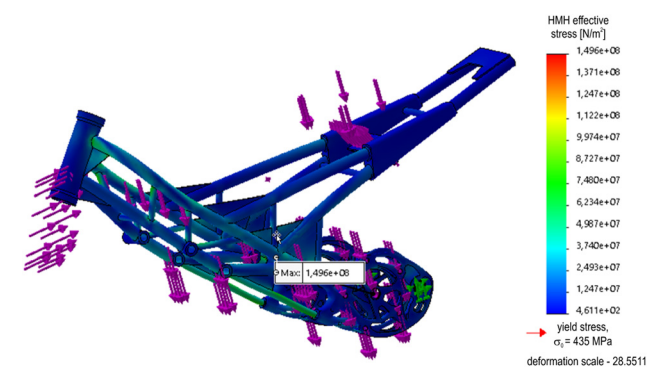


Figure 53: The HMH effective stress distribution estimated in the static braking test after modifications of the frame of the electric motorcycle.

157.3 MPa. Therefore, due to the assumed deviation of the allowable stresses, it allows the initial acceptance of the structure. The maximum displacement in the structure is slightly more than 4 mm (Figure 54). A significant part of the displacements is in the range from 0.5 to 2 mm, which is an acceptable result. Maximum deformations in the frame structure do not exceed 0.16%, which is also an expected result (Figure 55).

4 Summary, final conclusion, and presentation of a new industrial form

This study presents the use of the FEM in solving real engineering problems, using the example of an electric motorcycle design project. A simplified scheme of industrial design was presented, followed by an indication of how to use the capabilities of the selected CAD/CAM/CAE software in industrial design. Using concurrent design



Figure 52: Areas of modification in the static braking test for frame of electric motorcycle.

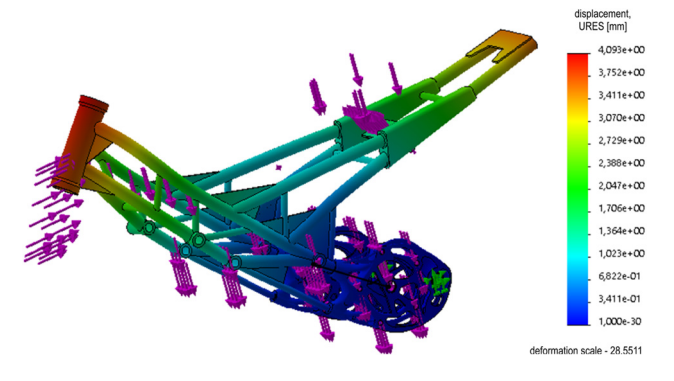


Figure 54: The distribution of the displacements in the static braking test after modifications of the frame of the electric motorcycle.

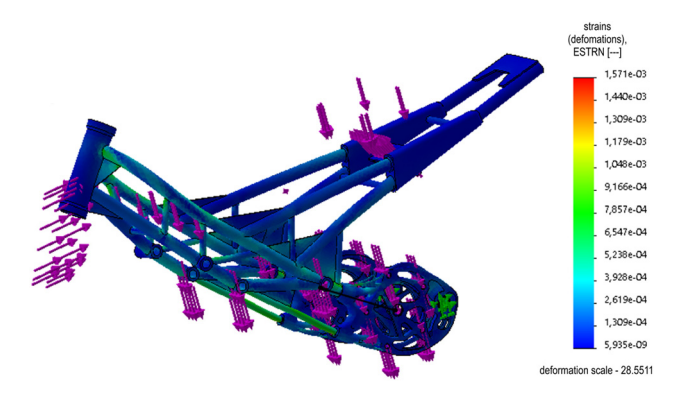


Figure 55: Distribution of the deformations (strains) in the static braking test after modifications of the frame of the electric motorcycle (the final form of the frame adopted in the design project).

based on the CAD system with the simultaneous use of CAE modules, the interdisciplinary of industrial design engineering was shown, which cannot exist without access to numerical methods.

Summing up the results presented in the study, they may be characterized by a significant discrepancy with the actual values in favor of the structure, due to the study of the model not connected to any other elements of the vehicle. On the basis of the results, it is possible to assume the acceptable strength of the structure, which means that the structural assumptions are met. The value of the weight of the frame after modifications is 5.54711 kg. Taking into account for minimum weight of welds and the use of additional reinforcing elements, the final mass was assumed as 6 kg. When evaluating the presented estimates, a number of assumed simplifications should be taken into account. In the simulations, the effect of welds was omitted, a homogeneous isotropic material was assumed. In some of the simulation tests, the friction force, air resistance, and elastic action of the front suspension, reducing the force acting on the frame, were omitted, assuming ideal component stiffness. As it is known, during numerical calculations, sometimes a small change in boundary conditions and load can lead to rapid



Figure 56: (a) Visualization of the new form of the electric motorcycle in plane (a) and in an axometric (b) projections.

changes in the obtained results. In the developed model of the frame, efforts were made to reflect all possible actual frame attachment and its load.

When conducting a series of numerical calculations using the SOLIDWORKS 2019 application [6], in each of the considered cases, higher-order SOLID finite elements with ten nodes and four Gaussian points were used. The developed divisions for subsequent mesh elements, in which the size of the finite element was often controlled, guaranteed convergence with the mesh filled with higherorder finite elements with 16 points of numerical integration.

In the electric motorcycle project discussed in this article, the close relation between CAD and CAE modules was used, looking for the best solution in the construction of the motorcycle frame. By conducting a series of numerical simulations based on the FEM and topological optimization, the final shape of the frame and the rear control arm mounting was presented. The designed structure was optimized in terms of mass and effective stress distributions determined from the HMH hypothesis. The resulting frame model was adapted to the design project (Figure 56). The study indicates the need to use the FEM and CAD/CAM/ CAE applications at almost every stage of engineering

During the preparation of the presented project, and next article, the authors considered carrying out some analyzes in other computational packages using the FEM (e.g., ADINA, ABAQUS, ANSYS). In the end, they stayed with the SOLIDWORKS 2019 application [6], which offers both work with the CAD, CAM, and CAE modules. Conducting the numerical analyzes presented in the previous paragraphs, the finite element model was initially optimized by selecting for all simulations the filling of discrete models with spatial finite elements of the SOLID type of higher order, with ten nodes and four Gaussian points. Developed for subsequent mesh elements, in which the size of the finite element was often controlled, they guaranteed convergence with the mesh filled with higher-order finite elements with 16 points of numerical integration. The use of ten nodal spatial finite elements of the SOLID type with only four points of numerical integration is fully justified in the case of low-strength structures, in which the effective stresses do not exceed the yield point. The analyzes carried out showed that the designed structure meets the assumptions, and the maximum effective stresses are lower than the allowable stresses, determined as 1/3 of the yield strength of the material used to make the frame.

The model of engineering work presented in this study, industrial design, solving engineering problems, construction problems, strength problems indicates the need for interdisciplinary education of engineers and an

interdisciplinary approach to the engineer's work in solving various issues. An example of this can be the manuscripts [20-24], in which the authors, by publishing their results, indicate interdisciplinary preparation for the role of an engineer, scientist, or researcher. In the study by Graba and Grycz [20], the FEM and structure topology analysis were used to propose a new industrial form of a flying drone. In the study by Kostka et al. [21], the aim of the scientific contribution is to point out the possibility of applicability of cylindrical shells with a constant elliptical cross-sectional shape for stability loss analysis. The authors present both experimental and numerical research work. In the study by Assimi et al. [22], authors present a genetic programming approach for simultaneous optimization of sizing and topology of truss structures. It aims to find the optimal cross-sectional areas and connections of the joints to achieve minimum weight in the search space. Kopas et al. [23] presented the analysis of selected mechanical properties of weld joints of AlMgSi07.F25 aluminum alloy based on experimental and numerical analysis. Blatnický et al. [24] presented a partial solution to the conception of the design of a manipulator for handling goods in particular difficult and limited operation conditions. It is considered to transport materials between two destinations.

To sum up, a good engineer must be highly interdisciplinary educated and prepared for scientific and research work. This is why we have prepared this article, to show our preparation and expectations for twenty-first century engineers.

Conflict of interest: Authors state no conflict of interest.

Data availability statement: Data sharing is not applicable to this article as no datasets were generated or analysed during the current study.

References

- Electric motorcycles and scooters. Available online: https://tiny.pl/ [1] wnvb2 (accessed on 28 November 2020).
- Zero Motorcycles. Available online: https://tiny.pl/wnvbb (accessed on 28 November 2020).
- Zero S. Available online: https://tiny.pl/wnvb3 (accessed on 28 November 2020).
- Grycz A. Preliminary design project for electric motorcycle. [4] Engineering Thesis, Kielce University of Technology - Faculty of Mechatronics and Mechanical Engineering - Department of Metrology and Non-conventional Manufacturing Methods, Kielce, Poland, 17 February 2021. (Polish).
- Tjalve E. Designing Industrial Forms. Arkady; Warsaw; 1985 (Polish).
- [6] Solid Works 2019 Documentation, Available online: https://tinv.pl/ wnvzm, (accessed on 21 February 2023).

- [7] Zienkiewicz OC, Taylor RL, Zhu JZ. The Finite Element Method: Its Basis and Fundamentals. 6th edn., Oxford: Elsevier; 2005. https:// tiny.pl/wnv3r (accessed on 22 February 2023).
- [8] Foale T. Motorcycle Handling And Chassis Design; Motochassis by Tony Foale. ISBN – 84-933286-3-4, Spain; 2002.
- [9] Lithium-ion battery. Available online: https://tiny.pl/wnbhp (accessed on 10 December 2020).
- [10] Analysis of Long-Range Interaction in Lithium-Ion Battery Electrodes. Available online https://tiny.pl/wnbh81 (accessed on 10 December 2020).
- [11] Kumar BR. Strength of materials. CRC Press. p. 300.
- [12] Bansal RK. A textbook of strength of materials: Mechanics of solids. New Delhi, India: Laxmi Publications; January 2012.
- [13] Niezgodziński ME, Niezgodziński T. Formulas, charts and strength tables. PWN Warsaw; 1977 (Polish).
- [14] Yoon GH. Topology optimization method with finite elements based on the k-ε turbulence model. Comput Methods Appl Mech Eng. 2020;361:112784. https://tiny.pl/wnbx2 (accessed on 22 February 2023).
- [15] Ramesh S, Handal R, Jensen MJ, Rusovici R. Topology optimization and finite element analysis of a jet dragster engine mount. Cogent Eng. 2020;7:1723821. doi: 10.1080/23311916.2020.1723821. https:// tiny.pl/wnbmq (accessed on 22 February 2023).
- [16] From Finite Element Analysis to Topology Optimization. Design Informatics Lab | School for Engineering of Matter, Transport and Energy. Arizona State University (2023), Available online: https:// tiny.pl/wnbm2 (accessed on 22 February 2023).
- [17] Lazarov BS. Topology optimization using multiscale finite element method for high-contrast media. Proceedings of International

- Conference on Large-Scale Scientific Computing; June 2014. p. 339–46. doi: 10.1007/978-3-662-43880-0_3. https://tiny.pl/wnbgq (accessed on 21 February 2023).
- [18] Huda N, Mursid O. Finite element analysis and topology optimization design of anchor mooring winch support bracket.
 6th International Conference on Marine Technology (SENTA 2021), IOP Conf. Series: Earth and Environmental Science.
 Vol. 972; 2022. p. 012078. doi: 10.1088/1755-1315/972/1/012078. https://tiny.pl/wnbgm (accessed on 21 February 2023).
- [19] Halliday D, Resnick R, Walker J. Fundamentals of physics. 8th edn. USA: John Wiley & Sons, Inc; 2008.
- [20] Graba M, Grycz A. Assessment of the mechanical properties of selected PLA filaments used in the UAV project. Materials. 2023:16:1194. doi: 10.3390/ma16031194.
- [21] Kostka J, Bocko J, Frankovský P, Delyová I, Kula T, Varga P. Stability loss analysis for thin-walled shells with elliptical cross-sectional area. Materials. 2021;14:5636. doi: 10.3390/ma14195636.
- [22] Assimi H, Jamali A, Nariman-zadeh N. Sizing and topology optimization of truss structures using genetic programming. Swarm Evolut Comput. 2017;37:90–103. doi: 10.1016/j.swevo.2017. 05.009.
- [23] Kopas P, Blatnický M, Sága M, Vaško M. Identification of mechanical properties of weld joints of AlMgSi07.F25 aluminium alloy. Anal Zavoda za Povijesne Znanosti Hrvatske Akademije Znanosti i Umjetnosti u Dubrovniku. 2017;56:99–102.
- [24] Blatnický M, Dižo J, Sága M, Gerlici J, Kuba E. Design of a mechanical part of an automated platform for oblique manipulation. Appl Sci. 2020;10:8467. doi: 10.3390/app10238467.